Received: 4 October 2021 | Revised: 20 January 2022 | Accepted: 23 February 2022

DOI: 10.1002/hbm.25823

RESEARCH ARTICLE

WILEY

Resting-state functional magnetic resonance imaging signal variations in aging: The role of neural activity

Xiaole Z. Zhong[1,2] | J. Jean Chen[1,2,3]

[1]Rotman Research Institute, Baycrest Health Sciences, Toronto, Ontario, Canada

[2]Department of Medical Biophysics, University of Toronto, Toronto, Ontario, Canada

[3]Institute of Biomedical Engineering, University of Toronto, Toronto, Ontario, Canada

Correspondence
J. Jean Chen, Rotman Research Institute, Baycrest Health Sciences, Toronto, ON, Canada.
Email: jchen@research.baycrest.org

Funding information
Canadian Institutes of Health Research, Grant/Award Number: 148398; Canadian Network for Research and Innovation in Machining Technology, Natural Sciences and Engineering Research Council of Canada, Grant/Award Number: 418443; Sandra Rotman Foundation

Abstract

Resting-state functional magnetic resonance imaging (rs-fMRI) has been extensively used to study brain aging, but the age effect on the frequency content of the rs-fMRI signal has scarcely been examined. Moreover, the neuronal implications of such age effects and age–sex interaction remain unclear. In this study, we examined the effects of age and sex on the rs-fMRI signal frequency using the Leipzig mind–brain–body data set. Over a frequency band of up to 0.3 Hz, we found that the rs-fMRI fluctuation frequency is higher in the older adults, although the fluctuation amplitude is lower. The rs-fMRI signal frequency is also higher in men than in women. Both age and sex effects on fMRI frequency vary with the frequency band examined but are not found in the frequency of physiological-noise components. This higher rs-fMRI frequency in older adults is not mediated by the electroencephalograph (EEG)-frequency increase but a likely link between fMRI signal frequency and EEG entropy, which vary with age and sex. Additionally, in different rs-fMRI frequency bands, the fMRI-EEG amplitude ratio is higher in young adults. This is the first study to investigate the neuronal contribution to age and sex effects in the frequency dimension of the rs-fMRI signal and may lead to the development of new, frequency-based rs-fMRI metrics. Our study demonstrates that Fourier analysis of the fMRI signal can reveal novel information about aging. Furthermore, fMRI and EEG signals reflect different aspects of age- and sex-related brain differences, but the signal frequency and complexity, instead of amplitude, may hold their link.

KEYWORDS
brain aging, electroencephalograph, fMRI signal amplitude, fMRI signal frequency, LEMON study, neurovascular coupling, resting-state fMRI, sex differences

1 | INTRODUCTION

Brain aging is a nebulous process that can involve many modulators and manifest through many markers of neuronal health. There have been established findings of cognitive (Harada, Natelson Love, & Triebel, 2013), morphological (Salat et al., 2004; Zhao et al., 2019), microstructural (Madden et al., 2012), vascular (Ungvari, Kaley, de Cabo, Sonntag, & Csiszar, 2010), and functional (Andrews-Hanna et al., 2007; Varangis, Habeck, Razlighi, & Stern, 2019) differences between healthy young and older adults. Moreover, resting-state functional connectivity is found to be higher in women (Hjelmervik, Hausmann, Osnes, Westerhausen, & Specht, 2014; Zhang

et al., 2016), and the rate of age-associated neuromorphological lower among women (Cowell et al., 1994; Edward Coffey et al., 1998; Gur et al., 1991), related primarily to female sex hormonal (estrogen) changes in aging (Colciago, Casati, Negri-Cesi, & Celotti, 2015; Resnick, Metter, & Zonderman, 1997; Rossetti, Cambiasso, Holschbach, & Cabrera, 2016; Zárate, Stevnsner, & Gredilla, 2017).

Understanding the effects of healthy aging on brain oscillations has long been a goal of aging research. Brain oscillations measured using electroencephalography such as electroencephalography (EEG) and magnetoencephalography (MEG) can provide measurements reflecting the age-effect underlying neuronal signals with power variation (see review in the study by Ishii et al., 2017) in each frequency band. EEG and MEG studies have also reported a reduction of neuronal activity frequency in mild cognitive impairment (Garcés et al., 2013). Hence, although electrophysiological measures of brain oscillations do not always have a clear one-to-one relationship to cognition, brain-oscillation dynamics are relevant to cognitive aging. Currently, the use of resting-state functional MRI (rs-fMRI) for mapping brain oscillations is rapidly growing. Brain variability (Garrett, Kovacevic, McIntosh, & Grady, 2010; Kumral et al., 2019), the amplitude of low-frequency fluctuations (ALFF) (Jia et al., 2020; Zou et al., 2008), and the resting-state fluctuation amplitude (RSFA) (Kannurpatti, Rypma, & Biswal, 2012) are all indicators of rs-fMRI oscillatory amplitude. Moreover, the ALFF and RSFA have both been found to vary with age (Tsvetanov et al., 2020; Yin et al., 2014).

Note that rs-fMRI fluctuation amplitude is associated with vascular (Tsvetanov et al., 2015), metabolic (Jiao et al., 2019), and cognitive influences (Garrett, Lindenberger, Hoge, & Gauthier, 2017; Takeuchi et al., 2017). Thus, the interpretation of rs-fMRI signal fluctuations has yet to be fully clarified. In this regard, one commonly investigated question is the relationship between fMRI and amplitudes of the EEG signals (de Munck et al., 2007; Goldman, Stern, Engel, & Cohen, 2002; Lu, Grova, Kobayashi, Dubeau, & Gotman, 2007). The EEG signal entropy (complexity) has also been associated with rs-fMRI functional connectivity (Liu, Song, Liang, Knöpfel, & Zhou, 2019; Wang et al., 2018). To date, it remains to be understood how age effects in EEG and fMRI signals are associated in the context of aging, which is a question that is central to the interpretation of rs-fMRI findings. Age-associated differences in neurovascular coupling are in turn key to understanding the age-related differences between the EEG-fMRI linkage, and this coupling could also vary with age (Tsvetanov, Henson, & Rowe, 2021).

The frequency content of the rs-fMRI signal can provide a novel set of markers of brain function. Indeed, frequency dependence of functional connectivity has been uncovered (Kalcher et al., 2014), and the frequency spectrum of the rs-fMRI signal has become increasingly studied to isolate dynamic neuronal and hemodynamic information (Yuen, Osachoff, & Chen, 2019). Given the multiple physiological changes that occur in aging, it is informative to incorporate frequency features into the study of aging using rs-fMRI as well. To date, the only work that has adopted this approach is by Yang et al. (Yang, Tsai, Lin, Peng, & Huang, 2018), who used the Hilbert transform to derive intrinsic modes of oscillation from the rs-fMRI signal. Their study found that the frequency band between 0.045 and 0.087 Hz is more strongly associated with cognitive scores, whereas lower frequencies are more likely to be driven by physiological processes such as spontaneous fluctuations in arterial carbon dioxide level at rest. This is in close agreement with findings by Yuen et al. in young adults using variational mode decomposition (Yuen et al., 2019). Furthermore, Yang et al. reported a widespread increase in the instantaneous frequencies in aging within the "cognitively driven" frequency band, with a less extensive increase at lower frequencies.

The previous work, while extremely novel and informative, has left some unanswered questions.

1. There is still very limited investigation into variations in the frequency of the rs-fMRI signal in aging and the age–sex interaction.
2. Given the known complexity of the signal and noise contributions to the rs-fMRI signal, including by intrinsic variations in carbon dioxide (CO_2) (Chang & Glover, 2009; Golestani, Chang, Kwinta, Khatamian, & Chen, 2015; Wise, Ide, Poulin, & Tracey, 2004), respiration (Birn, Diamond, Smith, & Bandettini, 2006; Chang & Glover, 2009; Golestani et al., 2015; Shams, LeVan, & Chen, 2021) and cardiac pulsation (Attarpour, Ward, & Chen, 2021; Chang et al., 2013; Falahpour, Refai, & Bodurka, 2013; Shmueli et al., 2007), the neuronal associations of the observed frequency shifts remain unclear. Hence, it is still unclear how EEG and fMRI are related in aging.
3. Given the widespread use of Fourier-transform based methods for studying rs-fMRI power distributions (Zou et al., 2008), it is important to clarify whether Fourier-based spectral decomposition can produce results to support the Hilbert-transform-based findings.

In this study, using data from the Leipzig mind–brain–body (LEMON) study (Babayan et al., 2019), we probe the above questions. This study is expected to lead to the improved use of rs-fMRI for studying aging brain dynamics.

2 | METHODS

2.1 | Participants

The "Leipzig Study for Mind-Body-Emotion Interaction" (LEMON, publicly available at http://fcon_1000.projects.nitrc.org/indi/retro/MPI_LEMON.html) (Babayan et al., 2019) dataset comprises 227 healthy subjects in two age groups. The older group is aged between 59 and 77 years old ($N = 74$, 37 females) while the younger group is between 20 and 40 years old ($N = 153$, 45 females). No participant reported a history of cardiovascular disease, psychiatric disease, neurological disorders, malignant disease, or medication/drug use that could affect the study. The study protocol conformed to the Declaration of Helsinki and was approved by the ethics committee at the medical faculty of the University of Leipzig (reference number 154/13-ff) (Table 1).

TABLE 1 Subject demographics

Attributes	Young	Old
N	134	51
Age (mean/*STDEV* of mean)	25.5 ± 3.4 years	66.9 ± 4.8 years
Male : Female (M:F) ratio	42:92	23:28

We performed additional quality control and excluded data sets that had incomplete data, mismatching sampling rates, image artifacts, excessive head movement, or excessive background noise. The final sample used in this study, with 185 subjects, includes 134 young (20–40 years old, 42 females) and 51 old subjects (59–77 years old, 23 females). Ages were only recorded by the LEMON study quinquennially (5-year steps), thus only the group means and *STDEV*s of the mean are provided. For the age distributions, see Figure A1 in Supplementary Materials. Furthermore, the education levels were provided in the German system (Hauptschule and above) and are equivalent to "high school" in North America across all subjects.

2.2 | Data acquisition

All data acquisitions are described in the LEMON publication (Babayan et al., 2019). The relevant sections are summarized below.

2.2.1 | Magnetic resonance imaging

Magnetic resonance imaging (MRI) was performed on a 3 T scanner (MAGNETOM Verio, Siemens Healthcare GmbH, Erlangen, Germany) equipped with a 32-channel head coil. Participants were informed to keep their eyes open while focusing on a low-contrast cross during the scan.

Structural T1-weighted image was acquired using an MP2RAGE sequence with parameters: TR = 5,000 ms, TE = 2.921 ms, TI1 = 700 ms, TI2 = 2,500 ms, FA1 = 4°, FA2 = 5°, bandwidth = 240 Hz/pixel, FOV = 256 mm, voxel size 1 mm isotropic, 176 slice encodes. Functional imaging was performed with a T2*-weighted gradient-echo EPI sequence, with TR = 1,400 ms, TE = 30 ms, flip angle = 69°, bandwidth = 1776 Hz/pixel, partial Fourier ⅞, voxel size 2.3 mm isotropic, 64 slices.

2.2.2 | Electroencephalograph

In a separate session, 16 min of resting-state EEG were recorded with BrainAmp MR-plus amplifiers using 62-channel (61 scale electrodes and 1 VEOG electrode below the right eye) active ActiCAP electrodes (both Brain Products GmbH, Gilching, Germany) attached according to the international standard 10-10 system and referenced to FCz. The ground electrode was located at the sternum and skin–electrode interface impedance was kept below 5 kΩ. The EEG signal is digitized at a sampling frequency of 2,500 Hz and amplitude resolution was set to 0.1 μV. The EEG session included a total of eight eyes-closed (EC) blocks and eight eyes-open (EO) blocks, each 60 s. During the EO blocks, subjects were asked to fixate on a black cross on a white background presented using the Presentation software (Version 16.5, Neurobehavioral System Inc., Berkley, CA, USA). As rsfMRI data were collected only in the EO condition, only EEG from the EO condition was used in the comparative analysis.

2.3 | rs-fMRI data preprocessing and analysis

The rs-fMRI processing strategy is summarized in Figure 1. fMRI preprocessing was implemented with tools from FSL (Jenkinson, Beckmann, Behrens, Woolrich, & Smith, 2012) and FreeSurfer (Fischl, 2012). The following steps were included in preprocessing: (a) 3D motion correction (FSL MCFLIRT), (b) slice-timing correction (FSL slicetimer), (c) brain extraction (FSL bet2 and FreeSurfer mri_watershed), (d) rigid body coregistration of functional data to the individual T1 image (FSL FLIRT), (e) regression of the mean signals from white-matter (WM) and cerebrospinal fluid (CSF) regions (fsl_glm), (f) bandpass filtering to obtain band 1 (0.01–0.1 Hz) and band 2 (0.1–0.3 Hz), (g) special normalization to MNI152 (Montreal Neurological Institute) standard space with spatial resolution 2 mm isotropic (FSL FLIRT and FNIRT), and (h) the data were spatially smoothed with 6 mm full-width half-maximum (FWHM) Gaussian kernel (FSL fslmaths). The two frequency bands are meant to capture fluctuations that are typically associated with neuronal activity (lower frequency) and physiological processes (higher frequency), informed by prior literature (Yang et al., 2018; Yuen et al., 2019). The band-pass filter was implemented using Matlab (327th order Kaiser band-pass FIR filter with respective passband) to ensure minimal overlap between the bands. The magnitude and phase responses of the filter are shown in Figure S2. Furthermore, the motion-correction parameters and the WM-CSF signals were saved as a surrogate for head-motion physiological noise traces for further analysis.

STDEV and central frequency were calculated within each voxel time series then segmented to 106 ROIs using the Harvard-Oxford subcortical and cortical atlas (Desikan et al., 2006) for the mediation and S-ratio analyses. In particular, the central frequency was calculated by the center-of-mass approach, expressed by Equation (1).

$$\text{frequency} = \frac{\sum_{i=0}^{m} P_i f_i}{\sum_{i=0}^{m} P_i}, \tag{1}$$

where P represents power, and f frequency, and ($i = 0,\ldots,m$) is the frequency index in the Fourier domain (m corresponds to the maximum frequency). This approach ensured greater robustness against noise than identifying a single peak frequency The amplitude envelope of each band's oscillations was extracted using the Hilbert transform (Rosenblum, Pikovsky, Kurths, Schäfer, & Tass, 2001) and then temporally smoothed by a kernel with a FWHM of 0.5 s.

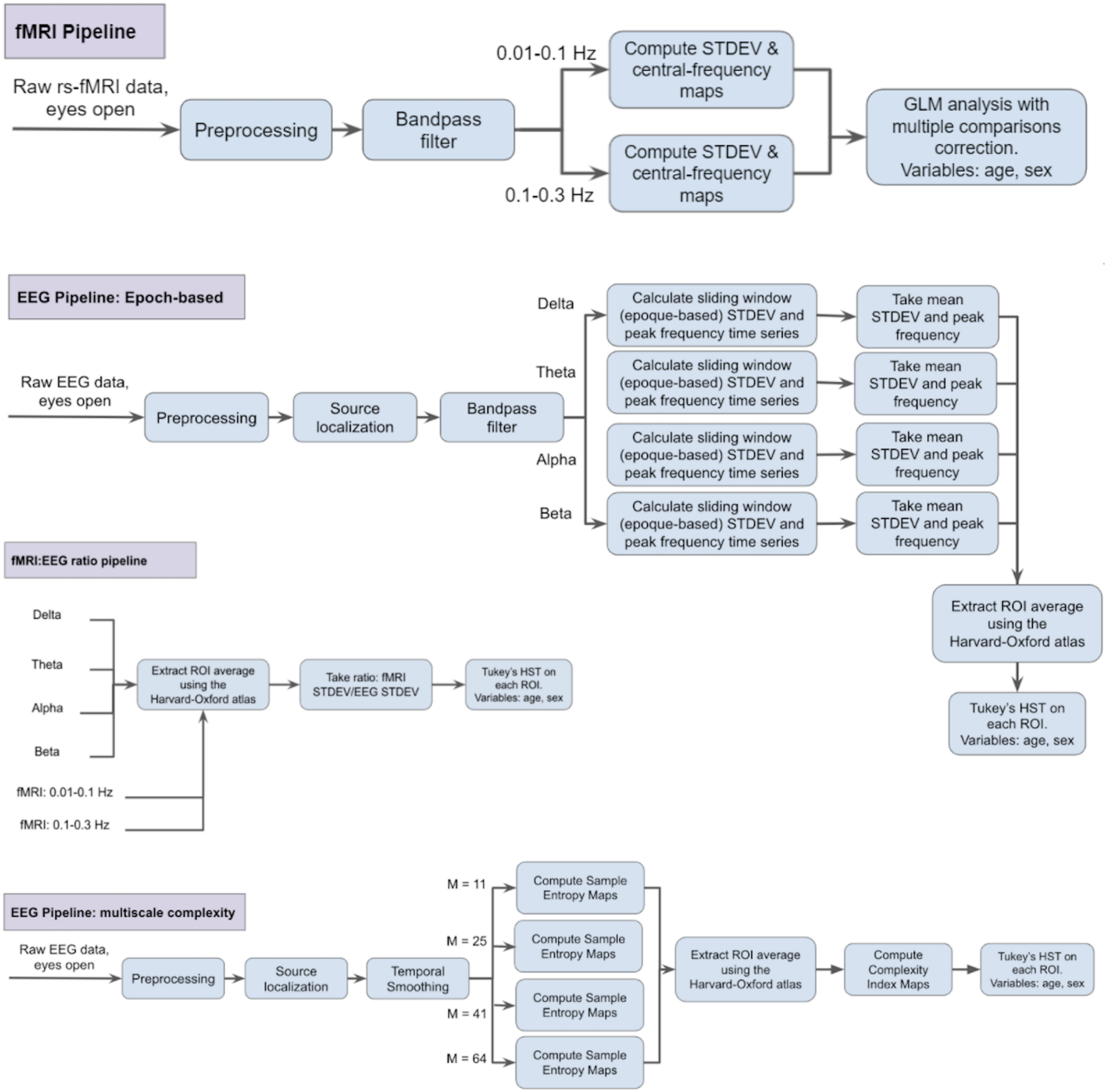

FIGURE 1 Overview of the analysis procedure. Two electroencephalograph (EEG) pipelines and one functional magnetic resonance imaging (fMRI) pipeline are used, as well as a ratios pipeline

2.4 | EEG data preprocessing and analysis

The EEG processing strategy is summarized in Figure 1. EEG preprocessing was conducted with EEGLAB (version 14.1.1bl; Delorme & Makeig, 2004) functions implemented in Matlab (The MathWorks Inc., Natick, Massachusetts, USA). The raw EEG data were down-sampled from 2,500 Hz to 250 Hz, band-pass filtered to 1–45 Hz with a fourth order back and forth Butterworth filter before being split into EO and EC conditions; 6.6% of the data were rejected by visual inspection, due to facial muscular tension and gross movements as well as artefactual channels. Furthermore, principal component analysis was used to reduce the dimensionality of the data to at least 30 principal components that explain 95% of the total variance. Then, using independent component analysis (Bell & Sejnowski, 1997), signal components related to physiological sources, for example, eye blinks, eye movements, residual ballistocardiograph artifacts, and muscle activity were further rejected. Preprocessed EEG signals were re-referenced to the common average and channel FCz was added as a normal channel.

The geometry of the source reconstruction model was based on the MNI/ICBM152 (International Consortium for Brain Mapping) standard anatomy. eLORETA (exact low-resolution brain electromagnetic tomography) implemented in the M/EEG toolbox of Hamburg (METH) (Haufe & Ewald, 2019) was used to compute the source distribution from the scalp EEG recordings. The lead field matrix was generated to relate 2,113 source voxels and 62 scalp electrodes. Singular-value decomposition of each voxel was used to determine the dominant orientation of the source signal.

2.4.1 | Band-limited approach

Band-pass filtering of the EEG signal was used to produce the well-known frequency bands of brain oscillations: delta (1–4 Hz), theta (4–8 Hz), alpha (8–12 Hz), and beta (12–30 Hz). We employed an epoch-based approach (Figure 1), whereby the standard deviation (STDEV) in each EEG band was calculated for sliding EEG epochs that match the TR of the fMRI data (1.4 s). This step allows us to match the temporal features in the EEG and fMRI time series and is analogous to the epoch-wise variability measure in task-based fMRI introduced by Garrett et al. (Garrett et al., 2010). The STDEV and peak EEG frequency were computed for each epoch. Power is reflected by STDEV of each source's smoothed time series, which are further averaged within 106 regions of interest (ROIs) as designated according to the Harvard-Oxford subcortical and cortical atlas (Desikan et al., 2006). Note that the STDEV is simply the square root of total spectral power (used for metrics such as the amplitude of low-frequency fluctuations; Zou et al., 2008). Subsequently, the epoch-based *STDEV* is calculated by the *STDEV* across all epoch-specific *STDEV*s. Peak frequencies were defined by the average of peak frequency in each epoch of corresponding EEG time series.

We also implemented a nonepoch analysis pipeline, in which EEG time series were used directly without epoch-matching to the fMRI data. The results are provided for reference only in Supplementary Materials Data S1.

2.4.2 | Multiscale approach

To simultaneously characterize multiple EEG bands, we computed multiscale entropy (MSE) (Costa, Goldberger, & Peng, 2002; Kosciessa, Kloosterman, & Garrett, 2020), which is the preeminent method for characterizing signal complexity. We chose four different scale factors, that is, $m = 64$, 41, 25, and 11 as MSE coarse-grain scale (Gao, Hu, Liu, & Cao, 2015). The order of permutation is set to 2 and the noise threshold is 0.5 relative to the STDEV of each band. Based on the MSE measures, we computed a complexity index (Costa, Goldberger, & Peng, 2005; Kang & Dingwell, 2016), that is, the area under the MSE curve, which indicates the amount of entropy over a range of time scales. We did not compute entropy in rs-fMRI data, due to its limited bandwidth.

2.4.3 | fMRI-EEG ratio

In prior literature, the relationship between EEG and fMRI signal amplitudes has been used to assess neurovascular coupling (Mullinger, Cherukara, Buxton, Francis, & Mayhew, 2017). In aging, the ratio between the fMRI and EEG task responses has been found to decrease, potentially reflecting changes in neurovascular coupling (Fabiani et al., 2014). Inspired by these prior works, we applied the same principle to the resting state to assess the effect of aging. The ratio of the rs-fMRI and EEG signal fluctuations is taken between signal pairs across the two fMRI frequency bands and four EEG bands. This measurement is intended to produce a surrogate of the vascular-neuronal fluctuation ratio in the resting state and is examined in the two fMRI frequency bands separately, as metric that could help provide context for the age and sex effect on fMRI signal frequency.

2.5 | Statistical methods

To investigate age and sex effect, EEG *STDEV*, peak frequency and complexity index from each 115 ROIs were examined by nonparametric analyses of covariance (ANCOVAs, type III) after outliers (data points outside of the 1.5-interquartile range) were removed. The significance of group differences was further tested by Tukey's honest significant difference (HSD) post hoc comparisons with a significance threshold of .05. All analyses were implemented in Matlab (The MathWorks Inc.).

BOLD fMRI central frequency and STDEV were tested for effects of age and sex with the ANOVA by used generalized linear model (GLM) implemented in FSL (Jenkinson et al., 2012) with significance threshold .05, corrected for multiple comparisons using randomize. In the age comparisons, sex was covaried, while in sex comparison, age was covaried. Subcortical region *STDEV* and central frequency were also examined by nonparametric analyses of covariance (ANCOVAs, type III) and Tukey's HSD post hoc comparisons to better investigate age and sex effects in these ROIs. Furthermore, effect sizes were calculated with Hedges' approach (Hedges, 1981) and threshold with significant region.

Two statistical approaches were used to probe the relationship between BOLD fMRI central frequency and EEG. The first approach used nonparametric analysis of covariance (ANCOVAs, type III) and Tukey's HSD post hoc test to analyze the age and sex effects on fMRI-EEG STDEV ratio. The second is a set of mediation analyses, as shown in Figure 2.

Based on the physiological relationship between neural activity and cerebral blood flow (Buxton, Wong, & Frank, 1998), the causality between electrophysiological and fMRI data can be reasonably established, which permits EEG variables to be used as mediators of fMRI variables even for cross-sectional data (Fairchild & McDaniel, 2017). Specifically, mediation pathway analysis (Hayes, 2013) was applied to investigate the association between EEG frequency and BOLD frequency, EEG STDEV and BOLD STDEV, as well as EEG complexity and BOLD frequency/amplitude in terms of

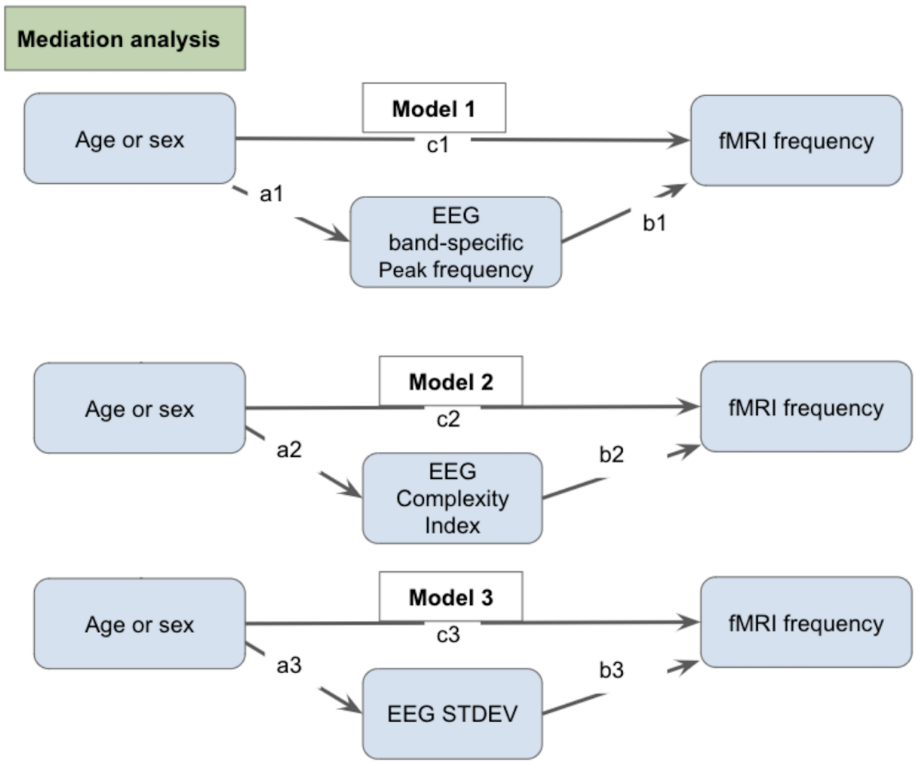

FIGURE 2 Models for the mediation analyses. We investigate the mediating effects of electroencephalograph (EEG) frequency (Model 1), complexity (Model 2), and amplitude (Model 3) on resting-state functional magnetic resonance imaging (rs-fMRI) frequency. The mediation coefficients a, b, and c represent indirect and direct effects. The independent variables are age and sex

age and sex effects. The models, summarized in Figure 2, were built in Matlab (The MathWorks Inc.) with the variational Bayesian analysis (VBA) toolbox (Daunizeau, Adam, & Rigoux, 2014). EEG parameters were set as a mediator while age or sex and BOLD parameters were the independent and dependent variables, respectively. The model was first built through Baron an Kenny's three-step mediation analysis (Baron & Kenny, 1986), and then examined by the Sobel test (Sobel, 1982) to determine whether the relationship between the independent variable and dependent variable is significantly reduced when including the mediator. The significance was declared when the *p* value from the Sobel test was lower than .05, corrected for false-discovery rate. Besides mediation analysis, correlation analysis was done between EEG *STDEV* and fMRI *STDEV*, EEG frequency and fMRI frequency as well as EEG complex index and fMRI frequency. Correlation results were threshold with the significant level .05 and corrected with FDR correction.

3 | RESULTS

3.1 | fMRI findings

3.1.1 | fMRI frequency versus age and sex

From Figure 3, it is evident that young adults have lower fMRI frequencies than older adults. The central frequency for the 0.01–0.1 Hz BOLD signal band is significantly higher in older adults in the superior frontal gyrus, insula, and superior temporal cortex for the cortical region, while the central frequency for the 0.1–0.3 Hz BOLD signal band significantly higher in older participants in more cortical regions (Figure 4). In the subcortical regions, older participants have higher rs-fMRI central frequency in the thalamus, caudate, putamen, pallidum, and hippocampus than younger participants, but only in the 0.1–0.3 Hz band (Figure 5a). Moreover, females have higher central frequencies in the occipital and parietal lobes (Figure 7) as well as the caudate (Figure 6) in the lower frequency component of the BOLD signal.

3.1.2 | fMRI amplitude versus age and sex

From Figure 3, it is evident that young adults have qualitatively higher fMRI signal amplitudes (as reflected by STDEV) and lower fMRI frequencies than older adults. Moreover, older adult STDEV maps display lower inter-regional variability than those of younger adults. rs-fMRI signal fluctuation amplitude is also significantly lower in older adults.

For the lower-frequency BOLD signal (0.01–0.1 Hz), younger adults show higher STDEV in the cingulate, superior frontal gyrus, middle frontal gyrus, and lingual gyrus for the cortical region (Figure 4). Compared with the 0.01–0.1 Hz BOLD signal, the BOLD signal at 0.1–0.3 Hz is associated with significant age effects in more ROIs, covering most of the cortical regions. For the subcortical regions, both frequency ranges show a significant age effect on the putamen (Figure 5b). Concerning the sex effect, only the lower-frequency BOLD showed higher amplitude in females in the frontal lobe (Figure 7). Lastly, spatial coregistration using linear and nonlinear methods yielded identical results. We did not assess age–sex interactions on the fMRI data, as the effect of sex on fMRI metrics was found to be negligible.

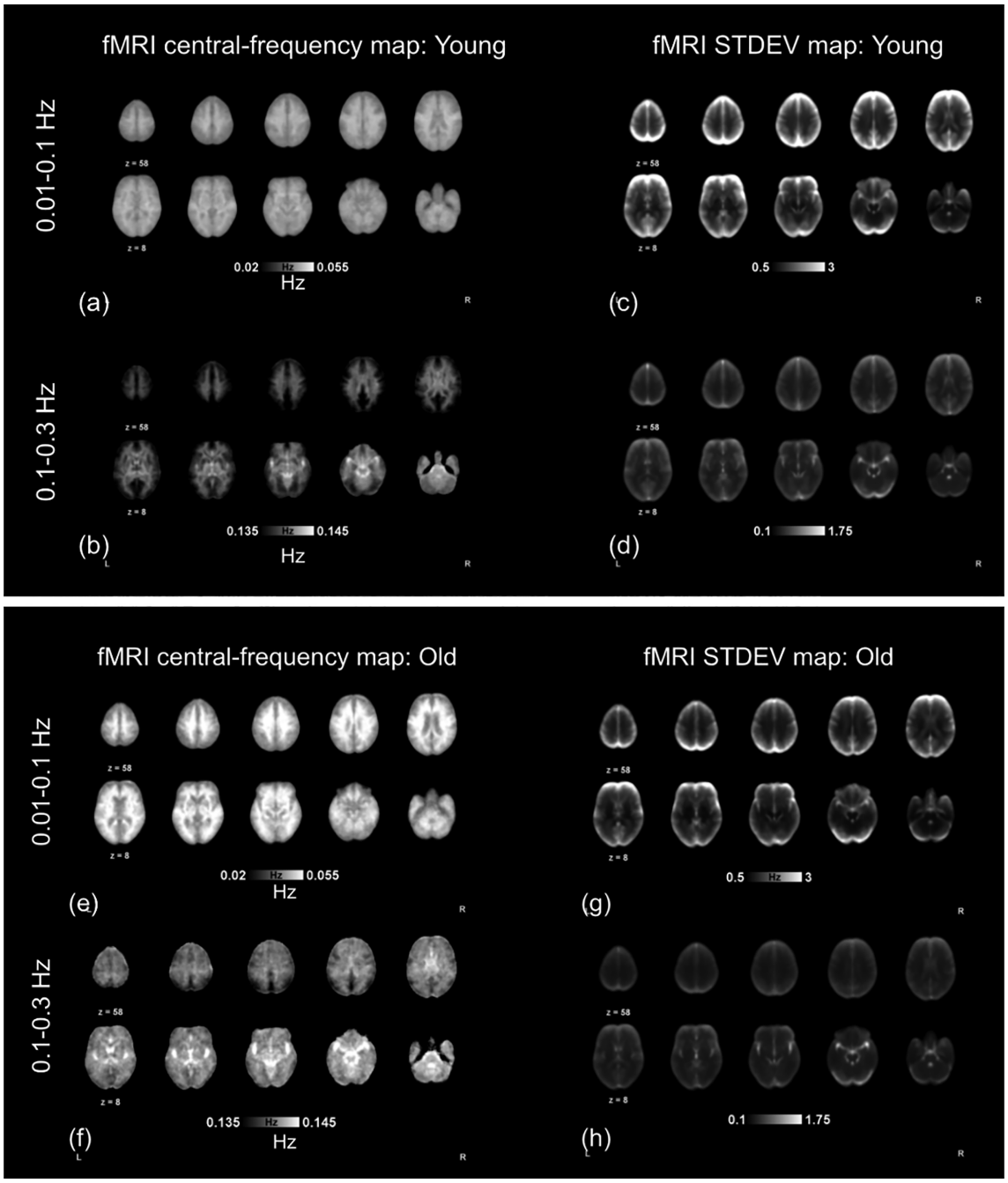

FIGURE 3 Mean resting-state functional magnetic resonance imaging (rs-fMRI) frequency and amplitude maps in young and old groups. The amplitude is given by the STDEV in units of %ΔBOLD. Cortical regions show higher STDEV than subcortical regions. Also young adults (a–d) have higher amplitude but lower frequency than older adults (e–h)

3.1.3 | The role of head motion and physiological noise

It has been suggested that sex and age differences of both fMRI STDEV and frequency could be attributed to differences in physiological confounds and motion effects between age and sex groups (van Dijk, Sabuncu, & Buckner, 2011). Concerning motion effects, we performed age and sex comparisons (ANCOVA with Tukey HSD post hoc test) on the magnitude and frequency with framewise motion estimates and did not find significant differences in our data (results not shown). Likewise, in regard to physiological confounds, we performed age and sex comparisons (ANCOVA with Tukey HSD post hoc test) to frequency and *STDEV* of white matter (WM) and cerebrospinal fluid (CSF) signals and found no significant age effect on the WM and CSF signals. We did, however, find that females have higher WM signal *STDEV* but lower frequency than males.

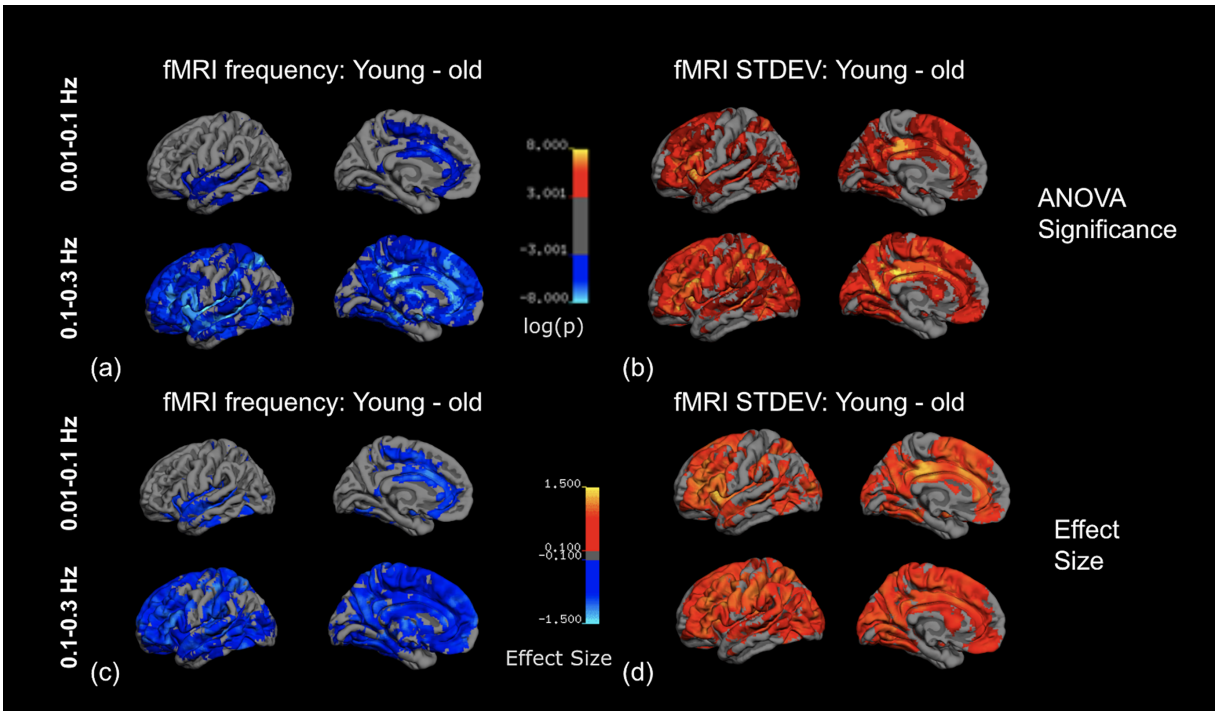

FIGURE 4 Resting-state functional magnetic resonance imaging (rs-fMRI) frequency and amplitude versus age. Only significantly different regions are shown in color. fMRI fluctuation frequency is higher in the older adults, also more extensively in the 0.1–0.3 Hz band. For reference, fMRI fluctuation amplitude is given as STDEV and is higher in the younger adults in both the 0.01–0.1 Hz and the 0.1–0.3 Hz bands, also with the 0.1–0.3 Hz band showing more widespread differences. All cases show significant differences in the cingulate cortex and paracentral cortex. Effect sizes range from 0.1 (small effect) to 1.5 (large effect)

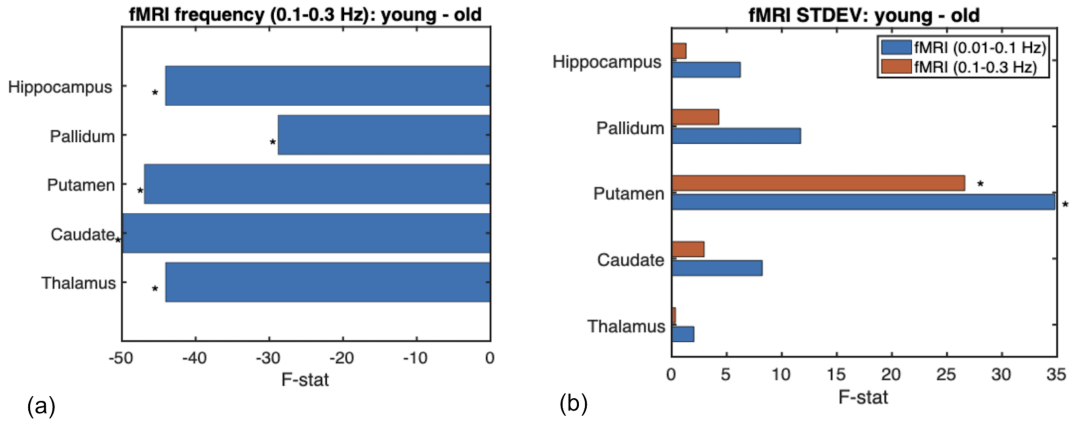

FIGURE 5 Resting-state functional magnetic resonance imaging (rs-fMRI) frequency and amplitude versus age: subcortical regions. (a) The fMRI frequency is higher in the older adults in all subcortical structures, but only in the 0.1–0.3 Hz band. (b) For reference, the fMRI signal amplitude is given as the STDEV and shows significant age effects (young > old) in the putamen in both fMRI frequency bands. Significance is indicated by asterisks (*)

3.2 | EEG findings

3.2.1 | EEG power versus age and sex

Tukey's HSD post hoc comparison shows that younger subjects exhibit lower EEG signal STDEV in the delta, theta, and alpha bands. The graphical distribution of the significant cortical age effects is shown in Figure 8. Older adults show lower EEG STDEV than younger adults in the alpha, theta, and delta bands. Significant main effects for the delta band are in the majority of cortical regions, more spatially restricted for the theta band. The beta band shows a different trend than the other three bands. Concerning the sex effect, females have

higher EEG *STDEV* than males in the beta, theta, and delta bands. See Figure 8 for detailed spatial distribution.

3.2.2 | EEG frequency versus age and sex

The graphical distribution of the significant cortical age effects includes those in the delta, theta, and the beta bands in the cortex (see Figure 9 for details). Delta band central frequency shows a significant reduction in the older adults, whereas theta and beta bands show significantly higher frequency in older adults. EEG central frequency only exhibits a significant age effect in cortical regions. The delta band is the only one that shows a significant sex effect for EEG frequency—females have higher frequency than males in the left and right frontal gyrus.

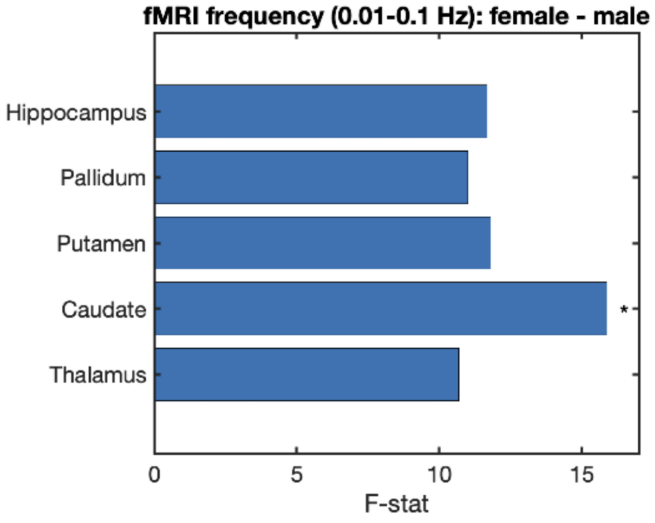

FIGURE 6 Resting-state functional magnetic resonance imaging (rs-fMRI) frequency and amplitude versus sex: subcortical regions. fMRI fluctuation frequency is higher in women only in the caudate's 0.01–0.1 Hz signal band. Significance is indicated by asterisks (*)

3.2.3 | EEG complexity versus age and sex

As shown in Figure 10, the multiscale EEG complexity index (CI) is lower in older adults in a wide swath of brain regions. It is also lower in females, which is most significant in the parietal lobe and in the left hemisphere than right hemisphere (Figure 10).

3.3 | Combining fMRI and EEG: The fMRI-EEG ratio

For the fMRI-EEG STDEV ratio, the distribution of ROIs showing significant age effects is shown in Figure 11. Statistical analysis reveals that the fMRI-alpha STDEV ratio in the 0.1–0.3 Hz fMRI frequency band is significantly higher in younger adults. Young adults also have higher fMRI-beta ratios in both the 0.01–0.1 Hz and 0.1–0.3 Hz bands and in more brain regions than for the fMRI-alpha ratio. The age effect is negligible for the fMRI-delta STDEV ratio in the 0.01–0.1 Hz band (one ROI, medial frontal cortex), the fMRI-alpha band in the 0.01–0.1 Hz frequency band (four ROIs in frontal and parietal regions), and the fMRI-theta STDEV ratio.

The spatial distribution showing significant sex effects is shown in Figure 12. Females are associated with significantly lower BOLD-EEG STDEV ratios than males in all frequency combinations (two fMRI frequencies vs. four EEG frequencies). Significant sex effects (female < male) are found in the STDEV ratios corresponding to all EEG bands, spanning the frontal, occipital, and paracentral regions. The effects are greatest for the beta band and more widespread for the 0.1–0.3 Hz fMRI-beta ratio.

Illustrated in Figure 13 is a side-by-side comparison of the fMRI frequency and fMRI-EEG STDEV ratio differences between young and old groups, to facilitate associations. Only the beta-band fMRI-EEG ratio is shown, as this is the band showing the most extensive age effects. For both parameters, age effects are more pronounced at higher frequency (0.1–0.3 Hz), and the majority of the effects are in the frontal part of the brain.

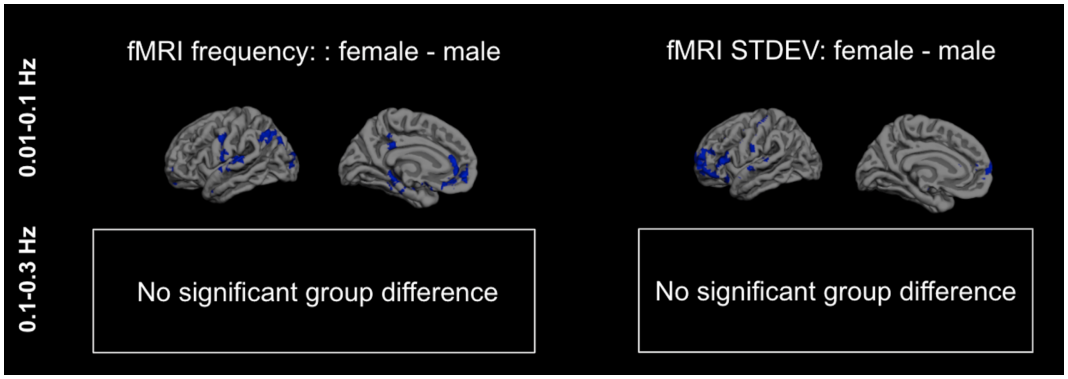

FIGURE 7 Resting-state functional magnetic resonance imaging (rs-fMRI) frequency and amplitude versus sex. All differences correspond to female minus male, and only statistically significant results are shown in color. There is minimal difference in rs-fMRI frequency between men and women

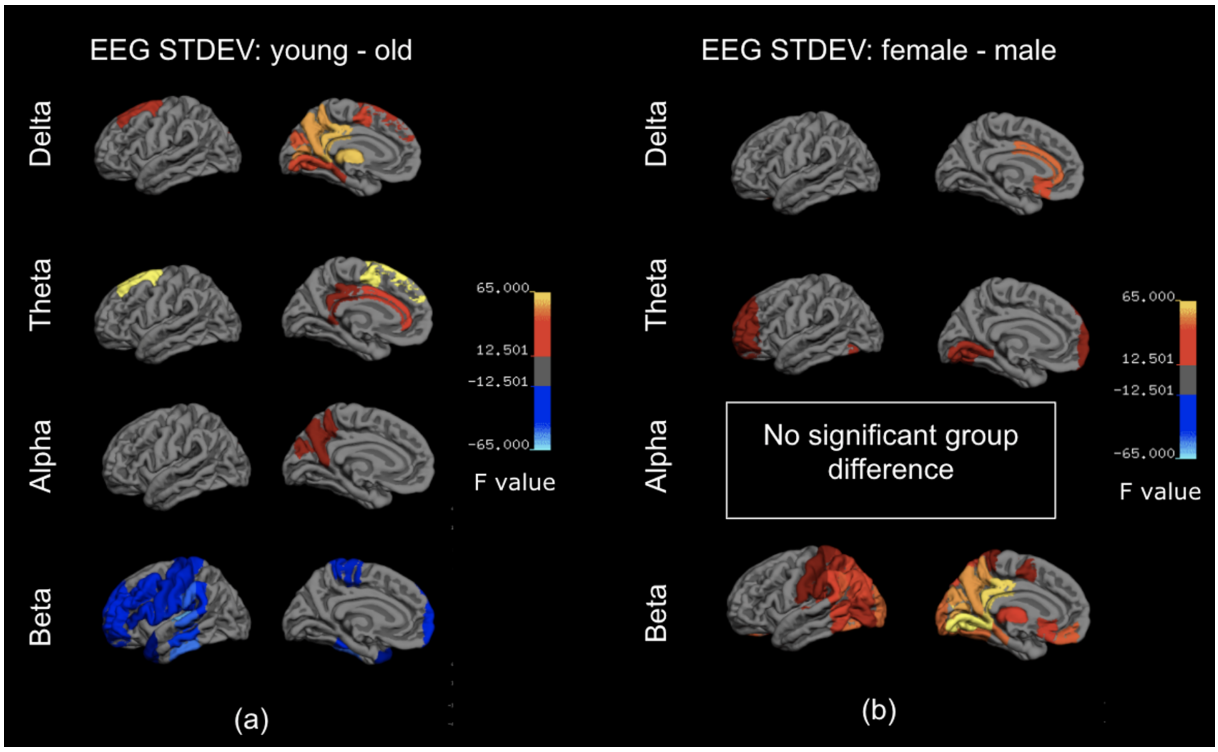

FIGURE 8 EEG STDEV versus age and sex. (a) All differences correspond to young minus old, and only statistically significant results are shown in color. Electroencephalograph (EEG) power is directly reflected by STDEV. (b) All differences correspond to females minus males, and only statistically significant results are shown in color. EEG power is computed as the signal *STDEV*

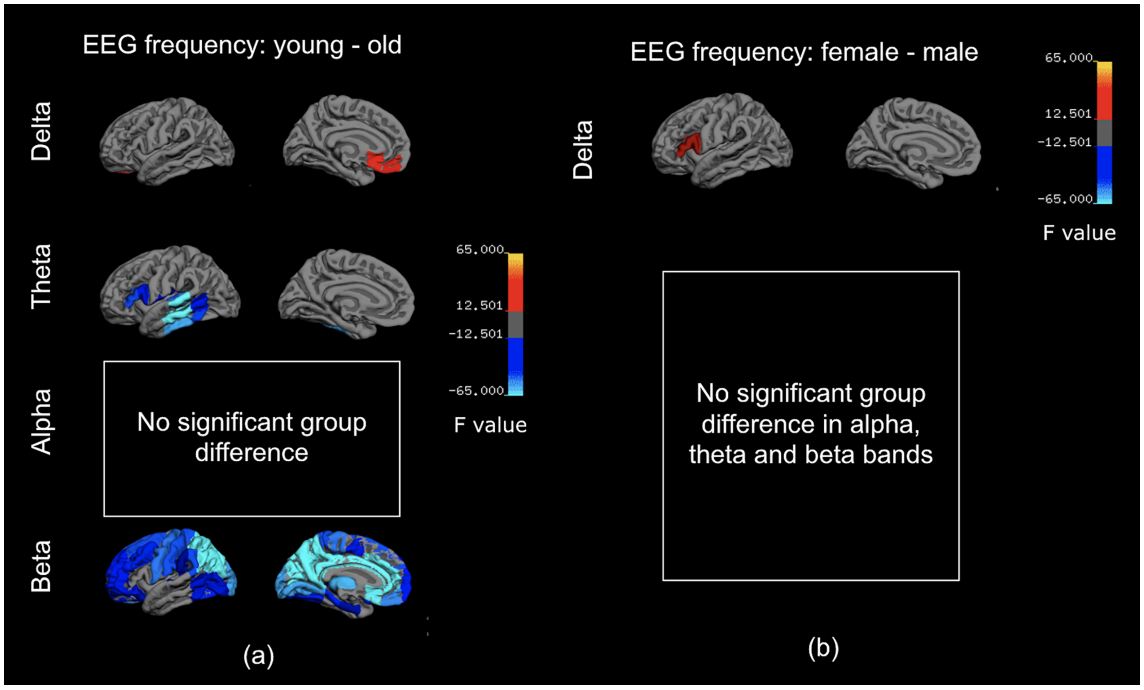

FIGURE 9 Electroencephalograph (EEG) frequency versus age and sex. (a) All differences correspond to young minus old, and only statistically significant results are shown in color. (b) All differences correspond to young minus old, and only statistically significant results are shown in color. There is minimal difference in EEG frequency between men and women (in the frontal gyrus)

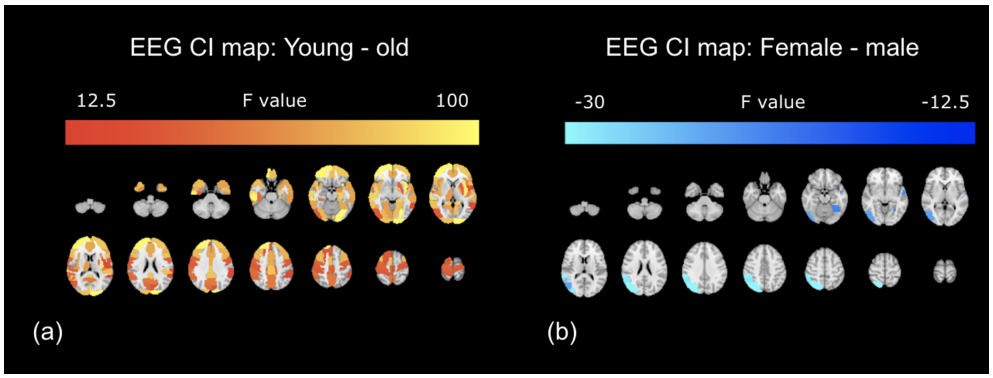

FIGURE 10 Electroencephalograph (EEG) complexity index (CI): age and sex effects. (a) Across all four EEG bands, EEG complexity is lower in the older adults, and the age effects are found across cortical regions. (b) Women are associated with lower EEG complexity in only one region of the brain (left parietal lobe)

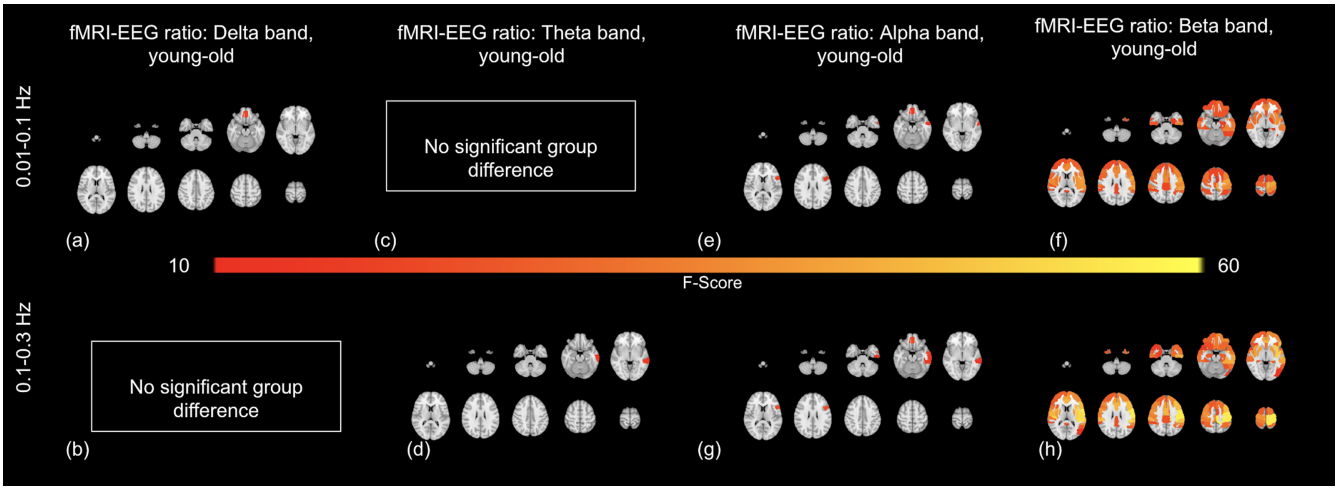

FIGURE 11 Resting-state functional magnetic resonance imaging (rs-fMRI)-electroencephalograph (EEG) STDEV ratio versus age segregated by fMRI frequency band. The fMRI-to-beta STDEV ratio exhibits the greatest age effects (young > old) (f, h). The effects are most pronounced in the 0.1–0.3 Hz range, and the affected regions span nearly the entire anterior cortex, also including subcortical regions such as the putamen and pallidum. The fMRI-to-theta ratio is lower in the young subjects in only the paracentral cortex

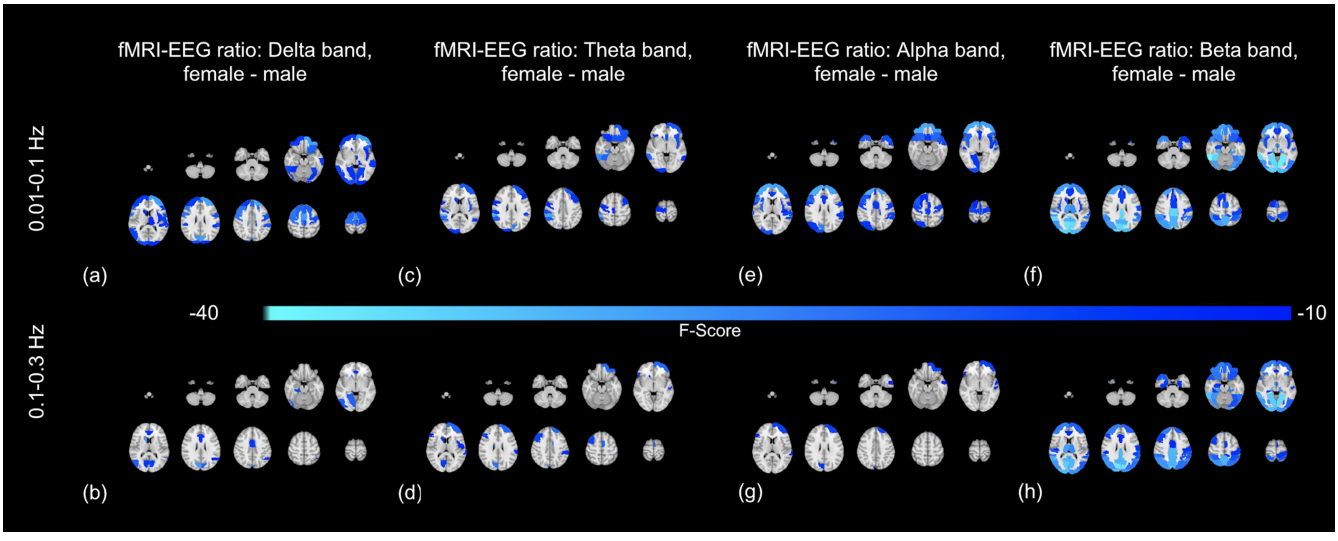

FIGURE 12 rs-fMRI-EEG STDEV ratio versus sex segregated by fMRI frequency band. Significant sex effects (female < male) are found in the ratios corresponding to all EEG bands, spanning the frontal, occipital and paracentral regions. The effects are greatest for the beta band, and more widespread for the 0.1–0.3 Hz fMRI-to-beta ratio

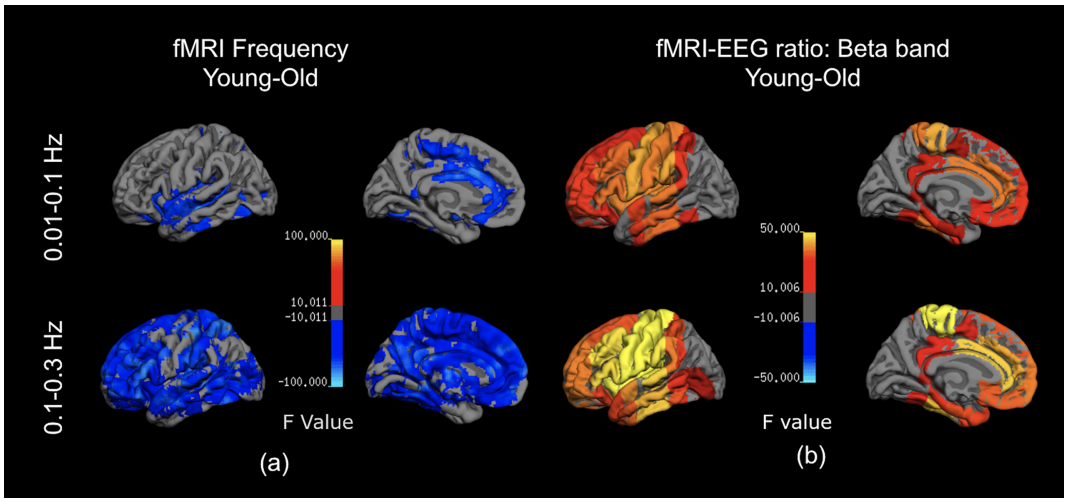

FIGURE 13 Comparison between rs-fMRI-EEG STDEV ratio versus age and fMRI frequency. The fMRI fluctuation frequency is higher in the older adults while the fMRI-to-beta STDEV ratio is higher in the younger adults. Age effects in both metrics are more pronounced in the 0.1–0.3 Hz frequency band, but both frequencies implicate the cingulate gyrus

The results of EEG and fMRI correlation analyses are summarized in Figure 14. Alpha and delta band EEG *SD* show positive correlations with *SD* in the 0.01–0.1 Hz fMRI band in the cingulate and occipital regions (Figure 14a,c), while the *SD* of the delta band is also correlated with *SD* in the higher fMRI frequency band (Figure 14b). Only in the EEG theta band are fMRI and EEG frequencies positively correlated, over the entire cortex with the exception of the middle-inferior frontal cortex (Figure 14d). Lastly, the EEG complexity index (Figure 14e) shows the most extensive significant correlation, being negatively correlated with SD in the higher fMRI frequency band.

3.4 | EEG mediation of fMRI frequency

3.4.1 | Mediation Model 1: EEG frequency mediating the age or sex differences in fMRI frequency

There is no evidence that the EEG peak frequency mediates the age or sex differences in the BOLD central frequency.

3.4.2 | Mediation Model 2: EEG complexity mediating the age or sex differences in fMRI frequency

The EEG complexity index (CI) is found to significantly mediate the age effect on BOLD frequency in both the 0.01–0.1 Hz and the 0.1–0.3 Hz bands. Regions involved include the insula, the cingulate gyrus, the operculum, the putamen, and the thalamus. For sex differences, EEG CI significantly mediates across wide swaths of the brain (see Table S1). This is despite there being minimal sex differences in EEG CI (Figure 9). Nonetheless, the mediation proportion remains limited (<2%).

3.4.3 | Mediation model 3: EEG STDEV mediating the age or sex differences in fMRI frequency

There is largely no evidence that EEG power (STDEV) mediates the age effect on the BOLD central frequency (see Table S3), except for the cuneal region, which shows partial mediation effect between EEG alpha band and fMRI 0.1–0.3 frequency band. For sex differences, EEG beta band power partially mediates four ROIs with BOLD frequency in 0.01–0.1 Hz bands and 0.1–0.3 Hz band, while the mediating effect by other EEG bands is negligible. (see Table S2).

4 | DISCUSSION

It is widely assumed that fMRI signal fluctuations represent neuronal fluctuations, but there is still limited work to clarify the neuronal contribution to fMRI signal variability. In particular, while most studies investigate rs-fMRI signal fluctuation amplitude (herein represented by STDEV), the frequency of the rs-fMRI signal, also rich in information, has been largely overlooked. In this study, we found that:

1. To address research question 1:
   a. The rs-fMRI frequency is lower in younger adults and in women.
   b. The rs-fMRI amplitude is greater in younger adults predominantly in the frequency >0.1 Hz.
2. To address research question 2:
   a. The rs-fMRI-EEG STDEV ratio is higher in the young adults and lower in women.
   b. The age and sex effects found in rs-fMRI fluctuation frequency are significantly mediated by EEG entropy.
3. To address research question 3:

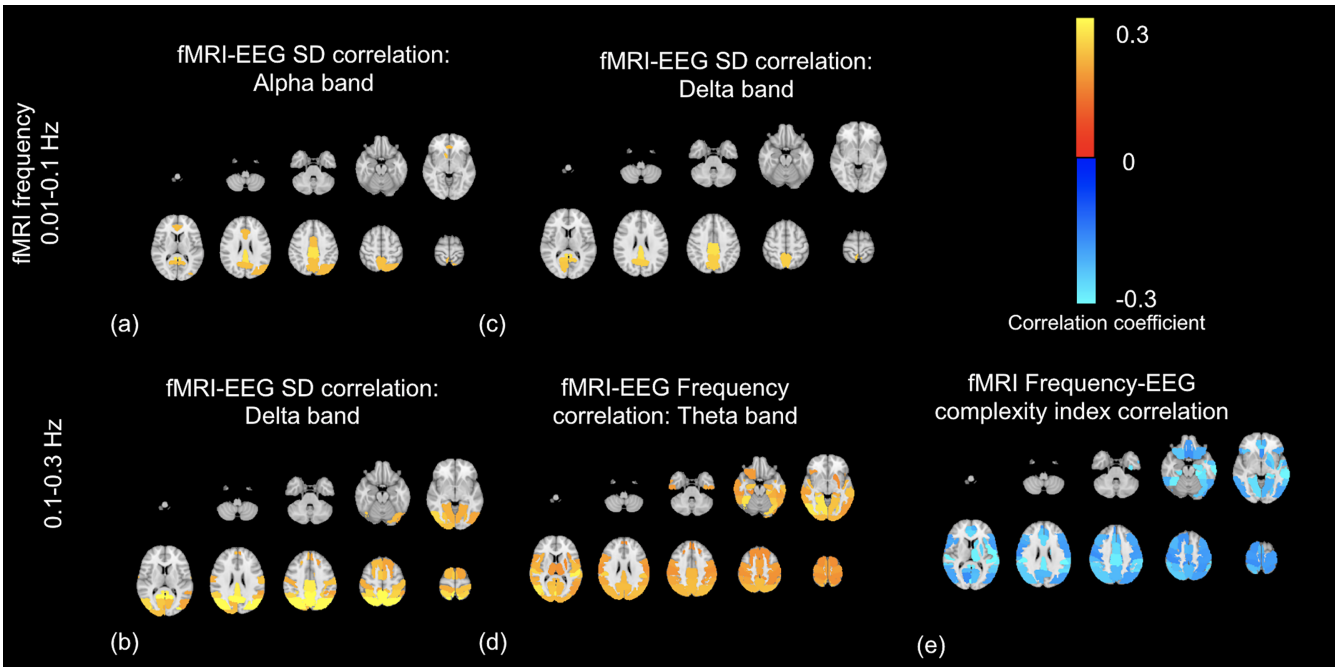

FIGURE 14 Correlations between fMRI and EEG metrics. Correlation results are threshold with the significance level .05 and corrected with FDR correction. *SD*, standard deviation

a. Fourier-based metrics are also able to reflect power-spectral changes previously reported using the Hilbert transform.

4.1 | fMRI frequency versus age and sex

The significance of BOLD fluctuation frequency has been largely uninvestigated. To date, the most relevant study is by Yang et al., who found aging-related IMF frequency increases in IMFs 2–5, which correspond to frequencies ranging below 0.087 Hz (Yang et al., 2018). This is consistent with our findings (for the 0.01–0.1 Hz band), demonstrating that Fourier-based metrics are able to reproduce frequency shifts previously shown in Hilbert-transform. However, we also found significant and widespread aging-related increases in the 0.1–0.3 Hz band, which is typically associated with an increased contribution from physiological processes (Yang et al., 2018). Interestingly, the most significant fMRI amplitude and frequency age effects, though in opposite directions, converge in the cingulate cortex.

We failed to detect a sex effect on fMRI frequency. Also, consistent with Kumral et al., we found no significant effect of sex on fMRI amplitude (Kumral et al., 2019). Conversely, the apparent increase in fMRI frequency with age, given the observation that overall fMRI signal fluctuation amplitude decreases with age in both frequency bands, point to a reduced contribution of low-frequency fluctuations to fMRI in older adults. In the 0.01–0.1 Hz band, the low-frequency contributions include arterial carbon dioxide (CO_2) fluctuations, respiratory variability and heart-rate variability (HRV) (Attarpour et al., 2021; Chang & Glover, 2009). Very-low frequency vascular oscillations measured using near-infrared spectroscopy have been found to decline in amplitude with age (Schroeter, Schmiedel, & von Cramon, 2004) and coincide in frequency with the resting vascular response to arterial CO_2 fluctuations (0.02–0.04 Hz) (Golestani et al., 2015; Liu et al., 2017). Also, low-frequency HRV, spanning 0.04–0.15 Hz, is found to decrease in aging (Rizzo et al., 1999), particularly in women (Moodithaya & Avadhany, 2012). Interestingly, the fMRI central-frequency increase for the 0.01–0.1 Hz band is restricted to the cingulate and frontal cortex, which are the very regions of reduced cerebrovascular reactivity reported in older adults (McKetton et al., 2018). The CVR-associated decrease of low-frequency hemodynamic response is consistent with our finding of an increase in fMRI central frequency. The 0.1–0.3 Hz band likely contains remnants of the neuronally driven fluctuations centered at 0.1 Hz. This is the frequency band typically used for functional-connectivity mapping, and a reduction in fMRI signal amplitude in this range would be consistent with the finding of lower EEG amplitude in older adults. Also in this frequency band are vasomotion and Mayer waves (Attarpour et al., 2021; Julien, 2006), which are found to decline in aging as well, consistent with reduced vascular smooth-muscle activity and increased vascular stiffening (Schroeter et al., 2004). Age-associated reductions in the frequency of vasomotion, which is found around 0.1 Hz, could also shift the vasomotion signal from the lower part of 0.1–0.3 Hz band to the higher part of 0.01–0.1 Hz band, giving the appearance of a higher central frequency of both bands (Vermeij, Meel-van den Abeelen, Kessels, van Beek, & Claassen, 2014).

Older adults are likely to express higher head motion (van Dijk et al., 2011), adding to the age-related shift of the fMRI signal toward higher frequency content. Nonetheless, we found no age effect (or sex effect) in the amplitude or frequency of head-motion

estimates. Nor did we find such effects in the amplitude and frequency of WM and CSF signals. Thus, the observed age differences are not expected to be driven by motion and physiological noise but are rather likely to indicate an age dependence on the neuronal contribution to the rs-fMRI signal. This is a finding that cannot be discerned from examining the rs-fMRI signal amplitude alone, as the amplitude metric does not distinguish contributions by different frequencies.

4.2 | fMRI signal amplitude versus age and sex

The BOLD signal fluctuation amplitude has been well studied in aging (Garrett, Kovacevic, McIntosh, & Grady, 2011; Garrett, McIntosh, & Grady, 2011; Guitart-Masip et al., 2016) and is thus not the focus of this study. Most studies of this kind, including the Kumral study, focus on the 0.01–0.1 Hz range, as it is most relevant to resting-state connectivity analysis. In this regard, our results echo the previous findings (Kumral et al., 2019): (a) a significant reduction in rs-fMRI signal amplitude in older adults across the cortical mantle; (b) no significant effect of sex. Also, like Grady and Garret (Grady & Garrett, 2014), we show that older adults have subdued inter-regional variability in their fMRI fluctuation amplitudes across the cortex as well as in the putamen, which has been associated with reduced cognitive performance and slower transition from rest to task states (Grady & Garrett, 2014).

The reproduction of the majority of Kumeral et al.'s findings on fMRI power is significant in establishing the plausibility of our other findings, especially given differences in our preprocessing pipelines. In our study, in addition to the typically studied 0.01–0.1 Hz frequency band, we also studied the 0.1–0.3 Hz band. This is inspired by the previous study by Yang et al. (Yang et al., 2018), whereby the rs-fMRI signal was categorized into high (0.087–0.2 Hz), low (0.045–0.087 Hz), and very low (0.045 Hz) frequency bands using the Hilbert–Huang Transform. In the "low-frequency band, Yang et al. found reduced fMRI amplitude in older adults. This is similar to our findings. As we found the fMRI signal in the 0.1–0.3 Hz frequency band to not produce the robust functional-connectivity patterns typically produced using the 0.01–0.1 Hz band (Yuen et al., 2019), we conclude, like Yang et al., that this high-frequency band is dominated by non-neuronal effects such as respiration and head motion. However, it is also worth noting that the rs-fMRI amplitude difference could be caused by both neuronal factors and physiological factors (e.g., neurovascular coupling).

4.3 | Age–sex interactions

Kumral et al. reported that older adults show higher beta EEG power, driven by the female subjects. As we used data from a very similar cohort, we expected the same finding. However, we found that men exhibit more age-related differences than women in the beta band, whereas women exhibit more age differences in the theta and delta bands. Conversely, in the beta and delta bands, older adults exhibit greater sex differences than young adults. Considering there is negligible rs-fMRI-related sex effect reported in our study with both frequency and amplitude metrics, it may be the case that rs-fMRI metrics display less age–sex interaction than EEG metrics. Nonetheless, the frontal region (Figure 7) shows sex differences in the 0.01–0.1 Hz band, warranting further investigation. Taken together, these results indicate the importance of considering the sex dependence of the aging process in EEG and fMRI studies. The differences with previous results could be attributed to differences in definitions of the EEG frequency bands. In Kumral et al.'s work, delta and beta bands are defined as 1–3 Hz and 15–25 Hz, respectively, whereas in our approach, delta is 1–4 Hz and beta is 12–30 Hz. The choice of a broader beta band is prompted by the large amount of beta power that still exists above 25 Hz, which may underlie the greater age difference in men and will require further investigation in our future work.

4.4 | Resting-state fMRI-EEG associations

4.4.1 | fMRI frequency versus EEG frequency and power

One might assume that resting-state fMRI and EEG frequency to be associated, given the consensus that fMRI signal and evoked EEG potentials can be associated through a hemodynamic response function (de Munck et al., 2007; Goldman et al., 2002). The EEG delta and theta bands exhibited higher and lower frequency in young adults, respectively. These observations are in part consistent with findings by Knyazeva et al., whereby low-frequency oscillations originating from the occipito-temporal regions in young adults move anteriorly with age (Knyazeva, Barzegaran, Vildavski, & Demonet, 2018). The beta band shows the strongest age effects (higher in older adults) in the cingulate and precuneus areas, which are generally associated with the default-mode network. The aging-related beta frequency elevation is consistent with the possible shift of sensory processing to high-frequency stimuli, leading to an increase in high-beta oscillations in older adults (Christov & Dushanova, 2016). Moreover, regions showing beta frequency increases appear to not overlap at all with regions showing beta power increase in aging. Chiang et al. reported frontal-occipital alpha frequency differences (lower alpha frequency in the frontal lobe) that may be altered by aging (Chiang, Rennie, Robinson, van Albada, & Kerr, 2011), which, as Knyazeva et al. described, amounts to a merging of high- and low-frequency alpha peaks in aging (Knyazeva et al., 2018). However, this did not translate into a frequency shift for alpha.

fMRI *SD* shows significant correlation with EEG *SD* in the alpha and delta bands, particularly in posterior brain regions (Figure 14). This could suggest the age-related variations in fMRI central frequency in these regions is a mixed effect of vascular and neuronal factors. Despite the neurovascular-coupling assumption, we found the mediation effect of EEG (amplitude or frequency) on fMRI fluctuation frequency to be negligible. An alternative determinant of fMRI frequency, as indicated by the study of Tsvetanov et al., could be

vascular reactivity (Tsvetanov et al., 2015). Based on observations in mild-cognitive impairment, aging is likely to be associated with a lower and slower vascular response (Richiardi et al., 2015). Moreover, arterial dysfunction has been observed in early stages of aging in the mouse model (Balbi et al., 2015). Nonetheless, Garrett et al. demonstrated that the age effect on the rs-fMRI signal is not solely due to vascular differences between age groups (Garrett et al., 2017). Thus, we conclude that the rs-fMRI frequency is a potential imaging marker that contains unique effects of aging and could be further helpful for improving rs-fMRI preprocessing.

4.4.2 | fMRI frequency versus EEG complexity

Interestingly, EEG complexity is found to significantly mediate age and sex effects on fMRI frequency. This is despite EEG complexity having no bearing on fMRI amplitude, albeit it is linked to functional connectivity (Wang et al., 2018). The complexity index, as a measure of entropy in the signal, is an additional dimension that does not fully covary with the amplitude and frequency measures, although recent work has suggested entropy can be inversely biased by signal power (Kosciessa et al., 2020). Our findings suggest that instead of EEG frequency or amplitude, a likely link between EEG and rs-fMRI is EEG complexity. More interestingly, this link is not observable through rs-fMRI amplitude but through its frequency dimension. Furthermore, the correlation maps shown in Figure 14 also confirms the significant association between fMRI frequency and EEG complexity index (albeit a negative association) in numerous brain regions. To the best of our knowledge, this possible complexity-frequency coupling has not been reported previously and opens the avenue for further applications of fMRI signal frequency content.

4.4.3 | fMRI frequency versus fMRI-EEG ratio

The fMRI-EEG STDEV ratio can help to enhance differences in the fMRI or EEG STDEV measures alone, and as mentioned earlier, can reflect certain aspects of neurovascular coupling. Younger adults are found to have higher fMRI-EEG STDEV ratios, analogous to findings based on the task response (Fabiani et al., 2014). The effects are most pronounced for the beta band, and the affected regions span nearly the entire anterior cortex as well as the putamen and pallidum, but not in the occipital region. This could be caused by the low prevalence of beta EEG power in posterior brain regions. Moreover, the age effect on the STDEV ratio is more pronounced in the 0.1–0.3 Hz range than in the 0.01–0.1 Hz range. This can be potentially interpreted as: (a) the neurovascular coupling ratio is known to be lower in older adults (Tarantini, Tran, Gordon, Ungvari, & Csiszar, 2017), consistent with the resting fMRI-EEG STDEV ratio being higher in young adults; (b) the age-difference in the fMRI STDEV (lower in older adults) is more pronounced in the 0.1–0.3 Hz band, likely driving the age effect in the fMRI-EEG STDEV ratio. Despite previous literature indicating higher noise content in the 0.1–0.3 Hz band, we did not find age effects in the WM-CSF and head-motion signals, suggesting that the age effects on the ratio may be attributed to factors such as vascular stiffness. Nonetheless, the age effects on the fMRI-EEG STDEV ratios overlap highly between the 0.01–0.1 Hz and 0.1–0.3 Hz bands, and one possible reason for this is that age-related fMRI STDEV reductions at 0.02–0.04 Hz (due to vascular reactivity decline) and reductions at 0.1 Hz (due to neural-activity decline) can coexist.

Some similarities are noted for the age effects on fMRI frequency and the fMRI-EEG STDEV ratio (for beta band EEG). In both cases, the age effects are more pronounced at higher frequencies (0.1–0.3 Hz), and the majority of the effects are in the frontal portion of the brain. This led us to explore possible connections between fMRI frequency and vascular reactivity in fMRI. As beta activity amplitude increases with age, so does the fMRI-EEG ratio. Is this mediated by high-frequency vascular oscillations (up to 0.3 Hz in our case)? The mechanisms underlying the fMRI frequency rise with age will be the focus of our future work.

4.5 | Limitations

As the LEMON EEG data do not contain gamma-band EEG, we limited our analysis to alpha, beta, delta, and theta bands. Moreover, the EEG and fMRI data were not acquired simultaneously. While this ensured superior data quality of both modalities, it precluded us from some interesting dynamic analyses. Furthermore, although EEG complexity is the strongest mediating factor for age effects among all EEG metrics, the mediation proportion is still modest (Table S1 and S2), warranting further investigations in larger samples. Finally, the sex ratios are different between young and old groups (age ratios are different between male and female groups). Nonetheless, we performed sex-specific age analysis (and age-specific sex analysis) to address sex- and age-related biases.

Moreover, it is increasingly recognized that physiological and psychological variability contribute to rs-fMRI and resting EEG signal (Anderson, Campbell, Amer, Grady, & Hasher, 2014; Tian, Chen, Xu, Yu, & Lei, 2020). Since EEG and fMRI data were acquired during different sessions, these sources of variability may play into intersubject variability in our observations.

5 | CONCLUSIONS

To conclude, the resting-state fMRI signal frequency is higher in older adults across different frequency bands. This does not appear to be mediated by EEG power or frequency. However, EEG complexity is found to significantly mediate age and sex effects in fMRI fluctuation frequency. Finally, the fMRI-EEG STDEV ratio shares many of the age effects observed in the fMRI signal frequency, and can be an interesting marker of the physiological process involved in brain aging, especially given its selective age sensitivity to the beta EEG band.

ACKNOWLEDGMENTS

The authors acknowledge funding support from the Canadian Institutes of Health Research (CIHR) and the Natural Sciences and Engineering Research Council of Canada (NSERC). The authors thank Dr. Jed Meltzer for helpful discussions. The authors are also grateful to Mr. Jeffrey Yu, Mr. Jacob Mattews, Mr. Nick Teller and Mr. Jordan Chad for proofreading.

ETHICS STATEMENT

The data is obtained from a publicly available data set (the LEMON study by the Max Planck Institute). Analysis of this data is approved by Baycrest Research Ethics Board.

PATIENT CONSENT STATEMENT

All participants who were included in the study are said to have provided written informed consent prior to any data acquisition for the study (including agreement to their data being shared anonymously) (Babayan, Nature, 2019).

DATA AVAILABILITY STATEMENT

All data described in this manuscript was obtained from the Leipzig mind- brain-body study. The data is available publicly at fcon_1000.projects.nitrc.org/indi/retro/MPI_LEMON.html. The code will be made available upon request.

ORCID

Xiaole Z. Zhong https://orcid.org/0000-0002-8641-5658
J. Jean Chen https://orcid.org/0000-0001-5469-7542

REFERENCES

Anderson, J. A. E., Campbell, K. L., Amer, T., Grady, C. L., & Hasher, L. (2014). Timing is everything: Age differences in the cognitive control network are modulated by time of day. *Psychology and Aging*, *29*(3), 648–657. https://doi.org/10.1037/a0037243

Andrews-Hanna, J. R., Snyder, A. Z., Vincent, J. L., Lustig, C., Head, D., Raichle, M. E., & Buckner, R. L. (2007). Disruption of large-scale brain systems in advanced aging. *Neuron*, *56*, 924–935. https://doi.org/10.1016/j.neuron.2007.10.038

Attarpour, A., Ward, J., & Chen, J. J. (2021). Vascular origins of low-frequency oscillations in the cerebrospinal fluid signal in resting-state fMRI: Validation using photoplethysmography. *Human Brain Mapping*, *42*(8), 2606–2622.

Babayan, A., Erbey, M., Kumral, D., Reinelt, J. D., Reiter, A. M. F., Röbbig, J., … Villringer, A. (2019). A mind-brain-body dataset of MRI, EEG, cognition, emotion, and peripheral physiology in young and old adults. *Scientific Data*, *6*, 180308. https://doi.org/10.1038/sdata.2018.308

Balbi, M., Ghosh, M., Longden, T. A., Jativa Vega, M., Gesierich, B., Hellal, F., … Plesnila, N. (2015). Dysfunction of mouse cerebral arteries during early aging. *Journal of Cerebral Blood Flow and Metabolism*, *35*, 1445–1453. https://doi.org/10.1038/jcbfm.2015.107

Baron, R. M., & Kenny, D. A. (1986). The moderator–mediator variable distinction in social psychological research: Conceptual, strategic, and statistical considerations. *Journal of Personality and Social Psychology*, *51*, 1173–1182.

Bell, A. J., & Sejnowski, T. J. (1997). The "independent components" of natural scenes are edge filters. *Vision Research*, *37*, 3327–3338.

Birn, R. M., Diamond, J. B., Smith, M. A., & Bandettini, P. A. (2006). Separating respiratory-variation-related fluctuations from neuronal-activity-related fluctuations in fMRI. *NeuroImage*, *31*, 1536–1548.

Buxton, R. B., Wong, E. C., & Frank, L. R. (1998). Dynamics of blood flow and oxygenation changes during brain activation: The balloon model. *Magnetic Resonance in Medicine*, *39*, 855–864. https://doi.org/10.1002/mrm.1910390602

Chang, C., & Glover, G. H. (2009). Relationship between respiration, end-tidal CO2, and BOLD signals in resting-state fMRI. *NeuroImage*, *47*, 1381–1393. https://doi.org/10.1016/j.neuroimage.2009.04.048

Chang, C., Metzger, C. D., Glover, G. H., Duyn, J. H., Heinze, H.-J., & Walter, M. (2013). Association between heart rate variability and fluctuations in resting-state functional connectivity. *NeuroImage*, *68*, 93–104. https://doi.org/10.1016/j.neuroimage.2012.11.038

Chiang, A. K. I., Rennie, C. J., Robinson, P. A., van Albada, S. J., & Kerr, C. C. (2011). Age trends and sex differences of alpha rhythms including split alpha peaks. *Clinical Neurophysiology*, *122*(8), 1505–1517. https://doi.org/10.1016/j.clinph.2011.01.040

Christov, M., & Dushanova, J. (2016). Functional correlates of the aging brain: Beta frequency band responses to age-related cortical changes. *International Journal of Neurorehabilitation*, *76*(2), 98–109. https://doi.org/10.4172/2376-0281.1000194

Colciago, A., Casati, L., Negri-Cesi, P., & Celotti, F. (2015). Learning and memory: Steroids and epigenetics. *The Journal of Steroid Biochemistry and Molecular Biology*, *150*, 64–85. https://doi.org/10.1016/j.jsbmb.2015.02.008

Costa, M., Goldberger, A. L., & Peng, C.-K. (2002). Multiscale entropy analysis of complex physiologic time series. *Physical Review Letters*, *89*(6), 068102. https://doi.org/10.1103/physrevlett.89.068102

Costa, M., Goldberger, A. L., & Peng, C.-K. (2005). Multiscale entropy analysis of biological signals. *Physical Review E*, *71*(2), 021906. https://doi.org/10.1103/physreve.71.021906

Cowell, P. E., Turetsky, B. I., Gur, R. C., Grossman, R. I., Shtasel, D. L., & Gur, R. E. (1994). Sex differences in aging of the human frontal and temporal lobes. *The Journal of Neuroscience*, *14*, 4748–4755.

Daunizeau, J., Adam, V., & Rigoux, L. (2014). VBA: A probabilistic treatment of nonlinear models for neurobiological and behavioural data. *PLoS Computational Biology*, *10*, e1003441. https://doi.org/10.1371/journal.pcbi.1003441

de Munck, J. C., Gonçalves, S. I., Huijboom, L., Kuijer, J. P. A., Pouwels, P. J. W., Heethaar, R. M., & Lopes da Silva, F. H. (2007). The hemodynamic response of the alpha rhythm: An EEG/fMRI study. *NeuroImage*, *35*, 1142–1151. https://doi.org/10.1016/j.neuroimage.2007.01.022

Delorme, A., & Makeig, S. (2004). EEGLAB: An open source toolbox for analysis of single-trial EEG dynamics including independent component analysis. *Journal of Neuroscience Methods*, *134*, 9–21. https://doi.org/10.1016/j.jneumeth.2003.10.009

Desikan, R. S., Ségonne, F., Fischl, B., Quinn, B. T., Dickerson, B. C., Blacker, D., … Killiany, R. J. (2006). An automated labeling system for subdividing the human cerebral cortex on MRI scans into gyral based regions of interest. *NeuroImage*, *31*, 968–980. https://doi.org/10.1016/j.neuroimage.2006.01.021

Edward Coffey, C., Lucke, J. F., Saxton, J. A., Ratcliff, G., Unitas, L. J., Billig, B., & Nick Bryan, R. (1998). Sex differences in brain aging: A quantitative magnetic resonance imaging study. *Archives of Neurology*, *55*, 169–179.

Fabiani, M., Gordon, B. A., Maclin, E. L., Pearson, M. A., Brumback-Peltz, C. R., Low, K. A., … Gratton, G. (2014). Neurovascular coupling in normal aging: A combined optical, ERP and fMRI study. *Neuroimage*, *85*(Pt 1), 592–607. https://doi.org/10.1016/j.neuroimage.2013.04.113

Fairchild, A. J., & McDaniel, H. L. (2017). Best (but oft-forgotten) practices: Mediation analysis. *The American Journal of Clinical Nutrition*, *105*, 1259–1271. https://doi.org/10.3945/ajcn.117.152546

Falahpour, M., Refai, H., & Bodurka, J. (2013). Subject specific BOLD fMRI respiratory and cardiac response functions obtained from global signal. *NeuroImage*, *72*, 252–264.

Fischl, B. (2012). FreeSurfer. *Neuroimage*, *62*, 774–781. https://doi.org/10.1016/j.neuroimage.2012.01.021

Gao, J., Hu, J., Liu, F., & Cao, Y. (2015). Multiscale entropy analysis of biological signals: A fundamental bi-scaling law. *Frontiers in Computational Neuroscience*, *9*, 64. https://doi.org/10.3389/fncom.2015.00064

Garcés, P., Vicente, R., Wibral, M., Pineda Pardo, J. A., Lopez, M. E., & Aurtenetxe, S. (2013). Brain-wide slowing of spontaneous alpha rhythms in mild cognitive impairment. *Frontiers in Aging Neuroscience*, *7*, 100.

Garrett, D. D., Kovacevic, N., McIntosh, A. R., & Grady, C. L. (2011). The importance of being variable. *The Journal of Neuroscience*, *31*(12), 4496–4503. https://doi.org/10.1523/JNEUROSCI.5641-10.2011

Garrett, D. D., Kovacevic, N., McIntosh, A. R., & Grady, C. L. (2010). Blood oxygen level-dependent signal variability is more than just noise. *The Journal of Neuroscience*, *30*, 4914–4921.

Garrett, D. D., Lindenberger, U., Hoge, R. D., & Gauthier, C. J. (2017). Age differences in brain signal variability are robust to multiple vascular controls. *Scientific Reports*, *7*, 10149.

Garrett, D. D., McIntosh, A. R., & Grady, C. L. (2011). Moment-to-moment signal variability in the human brain can inform models of stochastic facilitation now. *Nature Reviews. Neuroscience*, *12*, 612. https://doi.org/10.1038/nrn3061-c1

Goldman, R. I., Stern, J. M., Engel, J., & Cohen, M. S. (2002). Simultaneous EEG and fMRI of the alpha rhythm. *Neuroreport*, *13*(18), 2487–2492. https://doi.org/10.1097/00001756-200212200-00022

Golestani, A. M., Chang, C., Kwinta, J. B., Khatamian, Y. B., & Chen, J. J. (2015). Mapping the end-tidal CO_2 response function in the resting-state BOLD fMRI signal: Spatial specificity, test–retest reliability and effect of fMRI sampling rate. *NeuroImage*, *104*, 266–277.

Grady, C. L., & Garrett, D. D. (2014). Understanding variability in the BOLD signal and why it matters for aging. *Brain Imaging and Behavior*, *8*, 274–283. https://doi.org/10.1007/s11682-013-9253-0

Guitart-Masip, M., Salami, A., Garrett, D., Rieckmann, A., Lindenberger, U., & Bäckman, L. (2016). BOLD variability is related to dopaminergic neurotransmission and cognitive aging. *Cerebral Cortex*, *26*, 2074–2083. https://doi.org/10.1093/cercor/bhv029

Gur, R. C., Mozley, P. D., Resnick, S. M., Gottlieb, G. L., Kohn, M., Zimmerman, R., … Berretta, D. (1991). Gender differences in age effect on brain atrophy measured by magnetic resonance imaging. *Proceedings of the National Academy of Sciences of the United States of America*, *88*, 2845–2849. https://doi.org/10.1073/pnas.88.7.2845

Harada, C. N., Natelson Love, M. C., & Triebel, K. L. (2013). Normal cognitive aging. *Clinics in Geriatric Medicine*, *29*, 737–752.

Haufe, S., & Ewald, A. (2019). A simulation framework for benchmarking EEG-based brain connectivity estimation methodologies. *Brain Topography*, *32*, 625–642. https://doi.org/10.1007/s10548-016-0498-y

Hayes, A. F. (2013). *Introduction to mediation, moderation, and conditional process analysis: A regression-based approach*. New York, NY: Guilford.

Hedges, L. V. (1981). Distribution theory for Glass's estimator of effect size and related estimators. *Journal of Educational and Behavioral Statistics*, *6*, 107–128. https://doi.org/10.3102/10769986006002107

Hjelmervik, H., Hausmann, M., Osnes, B., Westerhausen, R., & Specht, K. (2014). Resting states are resting traits – An fMRI study of sex differences and menstrual cycle effects in resting state cognitive control networks. *PLoS One*, *9*(7), e103492. https://doi.org/10.1371/journal.pone.0103492

Ishii, R., Canuet, L., Aoki, Y., Hata, M., Iwase, M., Ikeda, S., … Ikeda, M. (2017). Healthy and pathological brain aging: From the perspective of oscillations, functional connectivity, and signal complexity. *Neuropsychobiology*, *75*, 151–161. https://doi.org/10.1159/000486870

Jenkinson, M., Beckmann, C. F., Behrens, T. E. J., Woolrich, M. W., & Smith, S. M. (2012). FSL. *Neuroimage*, *62*, 782–790. https://doi.org/10.1016/j.neuroimage.2011.09.015

Jia, X.-Z., Sun, J.-W., Ji, G.-J., Liao, W., Lv, Y.-T., Wang, J., … Zang, Y.-F. (2020). Percent amplitude of fluctuation: A simple measure for resting-state fMRI signal at single voxel level. *PLoS One*, *15*, e0227021. https://doi.org/10.1371/journal.pone.0227021

Jiao, F., Gao, Z., Shi, K., Jia, X., Wu, P., Jiang, C., … Zuo, C. (2019). Frequency-dependent relationship between resting-state fMRI and glucose metabolism in the elderly. *Frontiers in Neurology*, *10*, 566. https://doi.org/10.3389/fneur.2019.00566

Julien, C. (2006). The enigma of Mayer waves: Facts and models. *Cardiovascular Research*, *70*, 12–21. https://doi.org/10.1016/j.cardiores.2005.11.008

Kalcher, K., Boubela, R. N., Huf, W., Bartova, L., Kronnerwetter, C., Derntl, B., … Moser, E. (2014). The spectral diversity of resting-state fluctuations in the human brain. *PLoS One*, *9*, e93375.

Kang, H. G., & Dingwell, J. B. (2016). Differential changes with age in multiscale entropy of electromyography signals from leg muscles during treadmill walking. *PLoS One*, *11*, e0162034. https://doi.org/10.1371/journal.pone.0162034

Kannurpatti, S. S., Rypma, B., & Biswal, B. B. (2012). Prediction of task-related BOLD fMRI with amplitude signatures of resting-state fMRI. *Frontiers in Systems Neuroscience*, *6*, 7. https://doi.org/10.3389/fnsys.2012.00007

Knyazeva, M. G., Barzegaran, E., Vildavski, V. Y., & Demonet, J.-F. (2018). Aging of human alpha rhythm. *Neurobiology of Aging*, *69*, 261–273. https://doi.org/10.1016/j.neurobiolaging.2018.05.018

Kosciessa, J. Q., Kloosterman, N. A., & Garrett, D. D. (2020). Standard multiscale entropy reflects neural dynamics at mismatched temporal scales: What's signal irregularity got to do with it? *PLoS Computational Biology*, *16*, e1007885. https://doi.org/10.1371/journal.pcbi.1007885

Kumral, D., Şansal, F., Cesnaite, E., Mahjoory, K., Al, E., Gaebler, M., … Villringer, A. (2019). BOLD and EEG signal variability at rest differently relate to aging in the human brain. *Neuroimage*, *207*, 116373. https://doi.org/10.1016/j.neuroimage.2019.116373

Liu, M., Song, C., Liang, Y., Knöpfel, T., & Zhou, C. (2019). Assessing spatiotemporal variability of brain spontaneous activity by multiscale entropy and functional connectivity. *NeuroImage*, *198*, 198–220. https://doi.org/10.1016/j.neuroimage.2019.05.022

Liu, P., Li, Y., Pinho, M., Park, D. C., Welch, B. G., & Lu, H. (2017). Cerebrovascular reactivity mapping without gas challenges. *NeuroImage*, *146*, 320–326. https://doi.org/10.1016/j.neuroimage.2016.11.054

Lu, Y., Grova, C., Kobayashi, E., Dubeau, F., & Gotman, J. (2007). Using voxel-specific hemodynamic response function in EEG-fMRI data analysis: An estimation and detection model. *NeuroImage*, *34*, 195–203. https://doi.org/10.1016/j.neuroimage.2006.08.023

Madden, D. J., Bennett, I. J., Burzynska, A., Potter, G. G., Chen, N.-K., & Song, A. W. (2012). Diffusion tensor imaging of cerebral white matter integrity in cognitive aging. *Biochimica et Biophysica Acta*, *1822*, 386–400. https://doi.org/10.1016/j.bbadis.2011.08.003

McKetton, L., Sobczyk, O., Duffin, J., Poublanc, J., Sam, K., Crawley, A. P., … Mikulis, D. J. (2018). The aging brain and cerebrovascular reactivity. *NeuroImage*, *181*, 132–141. https://doi.org/10.1016/j.neuroimage.2018.07.007

Moodithaya, S., & Avadhany, S. T. (2012). Gender differences in age-related changes in cardiac autonomic nervous function. *Journal of Aging Research*, *2012*, 679345. https://doi.org/10.1155/2012/679345

Mullinger, K. J., Cherukara, M. T., Buxton, R. B., Francis, S. T., & Mayhew, S. D. (2017). Post-stimulus fMRI and EEG responses: Evidence for a neuronal origin hypothesised to be inhibitory. *NeuroImage*, *157*, 388–399. https://doi.org/10.1016/j.neuroimage.2017.06.020

Resnick, S. M., Metter, E. J., & Zonderman, A. B. (1997). Estrogen replacement therapy and longitudinal decline in visual memory. A possible protective effect? *Neurology*, *49*, 1491–1497. https://doi.org/10.1212/wnl.49.6.1491

Richiardi, J., Monsch, A. U., Haas, T., Barkhof, F., Van de Ville, D., Radü, E. W., … Haller, S. (2015). Altered cerebrovascular reactivity

velocity in mild cognitive impairment and Alzheimer's disease. *Neurobiology of Aging*, *36*, 33–41. https://doi.org/10.1016/j.neurobiolaging.2014.07.020

Rizzo, V., Villatico Campbell, S., Di Maio, F., Tallarico, D., Lorido, A., Petretto, F., … Carmenini, G. (1999). Spectral analysis of heart rate variability in elderly non-dipper hypertensive patients. *Journal of Human Hypertension*, *13*, 393–398. https://doi.org/10.1038/sj.jhh.1000810

Rosenblum, M., Pikovsky, A., Kurths, J., Schäfer, C., & Tass, P. A. (2001). Chapter 9 Phase synchronization: From theory to data analysis. In F. Moss & S. Gielen (Eds.), *Handbook of biological physics* (Vol. 4, pp. 279–321). Amsterdam, Netherlands: Elsevier.

Rossetti, M. F., Cambiasso, M. J., Holschbach, M. A., & Cabrera, R. (2016). Oestrogens and Progestagens: Synthesis and action in the brain. *Journal of Neuroendocrinology*, *28*(7). https://doi.org/10.1111/jne.12402

Salat, D. H., Buckner, R. L., Snyder, A. Z., Greve, D. N., Desikan, R. S. R., Busa, E., … Fischl, B. (2004). Thinning of the cerebral cortex in aging. *Cereb Cortex*, *14*, 721–730. https://academic.oup.com/cercor/article/14/7/721/375858

Schroeter, M. L., Schmiedel, O., & von Cramon, D. Y. (2004). Spontaneous low-frequency oscillations decline in the aging brain. *Journal of Cerebral Blood Flow & Metabolism*, *24*(10), 1183–1191. https://doi.org/10.1097/01.wcb.0000135231.90164.40

Shams, S., LeVan, P., & Chen, J. J. (2021). The neuronal associations of respiratory-volume variability in the resting state. *NeuroImage*, *230*, 117783.

Shmueli, K., van Gelderen, P., de Zwart, J. A., Horovitz, S. G., Fukunaga, M., Jansma, J. M., & Duyn, J. H. (2007). Low-frequency fluctuations in the cardiac rate as a source of variance in the resting-state fMRI BOLD signal. *NeuroImage*, *38*, 306–320. https://doi.org/10.1016/j.neuroimage.2007.07.037

Sobel, M. E. (1982). Asymptotic confidence intervals for indirect effects in structural equation models. *Sociological Methodology*, *13*, 290–312. http://www.jstor.org/stable/270723

Takeuchi, H., Taki, Y., Nouchi, R., Sekiguchi, A., Kotozaki, Y., Nakagawa, S., … Kawashima, R. (2017). Neural plasticity in amplitude of low frequency fluctuation, cortical hub construction, regional homogeneity resulting from working memory training. *Scientific Reports*, *7*, 1470. https://doi.org/10.1038/s41598-017-01460-6

Tarantini, S., Tran, C. H. T., Gordon, G. R., Ungvari, Z., & Csiszar, A. (2017). Impaired neurovascular coupling in aging and Alzheimer's disease: Contribution of astrocyte dysfunction and endothelial impairment to cognitive decline. *Experimental Gerontology*, *94*, 52–58. https://doi.org/10.1016/j.exger.2016.11.004

Tian, Y., Chen, X., Xu, D., Yu, J., & Lei, X. (2020). Connectivity within the default mode network mediates the association between chronotype and sleep quality. *Journal of Sleep Research*, *29*, e12948. https://doi.org/10.1111/jsr.12948

Tsvetanov, K. A., Henson, R. N. A., Jones, P. S., Mutsaerts, H., Fuhrmann, D., Tyler, L. K., & Cam-CAN, R. J. B. (2020). The effects of age on resting-state BOLD signal variability is explained by cardiovascular and cerebrovascular factors. *Psychophysiology*, *58*(7), e13714. https://doi.org/10.1111/psyp.13714

Tsvetanov, K. A., Henson, R. N. A., & Rowe, J. B. (2021). Separating vascular and neuronal effects of age on fMRI BOLD signals. *Philosophical Transactions of the Royal Society of London. Series B, Biological Sciences*, *376*, 20190631. https://doi.org/10.1098/rstb.2019.0631

Tsvetanov, K. A., Henson, R. N. A., Tyler, L. K., Davis, S. W., Shafto, M. A., Taylor, J. R., … Cam-Can, R. J. B. (2015). The effect of ageing on fMRI: Correction for the confounding effects of vascular reactivity evaluated by joint fMRI and MEG in 335 adults. *Human Brain Mapping*, *36*, 2248–2269. https://doi.org/10.1002/hbm.22768

Ungvari, Z., Kaley, G., de Cabo, R., Sonntag, W. E., & Csiszar, A. (2010). Mechanisms of vascular aging: New perspectives. *The Journals of Gerontology. Series A, Biological Sciences and Medical Sciences*, *65*, 1028–1041. https://doi.org/10.1093/gerona/glq113

van Dijk, K. R. A., Sabuncu, M. R., & Buckner, R. L. (2011). The influence of head motion on intrinsic functional connectivity MRI. *NeuroImage*, *59*, 431–438.

Varangis, E., Habeck, C. G., Razlighi, Q. R., & Stern, Y. (2019). The effect of aging on resting state connectivity of predefined networks in the brain. *Frontiers in Aging Neuroscience*, *11*, 234. https://doi.org/10.3389/fnagi.2019.00234

Vermeij, A., Meel-van den Abeelen, A. S. S., Kessels, R. P. C., van Beek, A. H. E. A., & Claassen, J. A. H. R. (2014). Very-low-frequency oscillations of cerebral hemodynamics and blood pressure are affected by aging and cognitive load. *NeuroImage*, *85*(Pt 1), 608–615. https://doi.org/10.1016/j.neuroimage.2013.04.107

Wang, D. J. J., Jann, K., Fan, C., Qiao, Y., Zang, Y.-F., Lu, H., & Yang, Y. (2018). Neurophysiological basis of multi-scale entropy of brain complexity and its relationship with functional connectivity. *Frontiers in Neuroscience*, *12*, 352. https://doi.org/10.3389/fnins.2018.00352

Wise, R. G., Ide, K., Poulin, M. J., & Tracey, I. (2004). Resting fluctuations in arterial carbon dioxide induce significant low frequency variations in BOLD signal. *NeuroImage*, *21*, 1652–1664.

Yang, A. C., Tsai, S.-J., Lin, C.-P., Peng, C.-K., & Huang, N. E. (2018). Frequency and amplitude modulation of resting-state fMRI signals and their functional relevance in normal aging. *Neurobiology of Aging*, *70*, 59–69. https://doi.org/10.1016/j.neurobiolaging.2018.06.007

Yin, S., Zhu, X., Li, R., Niu, Y., Wang, B., Zheng, Z., … Li, J. (2014). Intervention-induced enhancement in intrinsic brain activity in healthy older adults. *Scientific Reports*, *4*, 7309. https://doi.org/10.1038/srep07309

Yuen, N. H., Osachoff, N., & Chen, J. J. (2019). Intrinsic frequencies of the resting-state fMRI signal: The frequency dependence of functional connectivity and the effect of mode mixing. *Frontiers in Neuroscience*, *13*, 900. https://doi.org/10.3389/fnins.2019.00900

Zárate, S., Stevnsner, T., & Gredilla, R. (2017). Role of estrogen and other sex hormones in brain aging neuroprotection and DNA repair. *Frontiers in Aging Neuroscience*, *9*, 430. https://doi.org/10.3389/fnagi.2017.00430

Zhang, C., Cahill, N. D., Arbabshirani, M. R., White, T., Baum, S. A., & Michael, A. M. (2016). Sex and age effects of functional connectivity in early adulthood. *Brain Connectivity*, *6*(9), 700–713. https://doi.org/10.1089/brain.2016.0429

Zhao, L., Matloff, W., Ning, K., Kim, H., Dinov, I. D., & Toga, A. W. (2019). Age-related differences in brain morphology and the modifiers in middle-aged and older adults. *Cerebral Cortex*, *29*, 4169–4193. https://doi.org/10.1093/cercor/bhy300

Zou, Q. H., Zhu, C. Z., Yang, Y., Zuo, X. N., Long, X. Y., Cao, Q. J., … Zang, Y. F. (2008). An improved approach to detection of amplitude of low-frequency fluctuation (ALFF) for resting-state fMRI: Fractional ALFF. *Journal of Neuroscience Methods*, *172*, 137–141. http://www.ncbi.nlm.nih.gov/pubmed/18501969

SUPPORTING INFORMATION

Additional supporting information may be found in the online version of the article at the publisher's website.

How to cite this article: Zhong, X. Z., & Chen, J. J. (2022). Resting-state functional magnetic resonance imaging signal variations in aging: The role of neural activity. *Human Brain Mapping*, *43*(9), 2880–2897. https://doi.org/10.1002/hbm.25823